nature

THE INTERN[illegible]RNAL OF SCI[illegible]

Social support

How oxytocin helps make social interactions rewarding PAGE 179

BIODIVERSITY

TINKER, TAILOR, HERPETOLOGIST

Frog hunting with a dash of espionage

PAGE 150

MEDICAL RESEARCH

WHOSE DISEASE IS IT ANYWAY?

The value of patient involvement in research

PAGE 160

BIOGRAPHY

THE BRIEF-HISTORY MAN

Stephen Hawking — the book and the movie

PAGE 162

NATURE.COM/NATURE

12 September 2013 £10

Vol. 501, No. 7466

9 770028 083095 28

ARTICLE

doi:10.1038/nature12518

Social reward requires coordinated activity of nucleus accumbens oxytocin and serotonin

Gül Dölen[1]†, Ayeh Darvishzadeh[1], Kee Wui Huang[1] & Robert C. Malenka[1]

Social behaviours in species as diverse as honey bees and humans promote group survival but often come at some cost to the individual. Although reinforcement of adaptive social interactions is ostensibly required for the evolutionary persistence of these behaviours, the neural mechanisms by which social reward is encoded by the brain are largely unknown. Here we demonstrate that in mice oxytocin acts as a social reinforcement signal within the nucleus accumbens core, where it elicits a presynaptically expressed long-term depression of excitatory synaptic transmission in medium spiny neurons. Although the nucleus accumbens receives oxytocin-receptor-containing inputs from several brain regions, genetic deletion of these receptors specifically from dorsal raphe nucleus, which provides serotonergic (5-hydroxytryptamine; 5-HT) innervation to the nucleus accumbens, abolishes the reinforcing properties of social interaction. Furthermore, oxytocin-induced synaptic plasticity requires activation of nucleus accumbens 5-HT1B receptors, the blockade of which prevents social reward. These results demonstrate that the rewarding properties of social interaction in mice require the coordinated activity of oxytocin and 5-HT in the nucleus accumbens, a mechanistic insight with implications for understanding the pathogenesis of social dysfunction in neuropsychiatric disorders such as autism.

The mesocorticolimbic (MCL) circuit, implicated in encoding the rewarding properties of addictive drugs, is likely to have evolved to motivate behaviours that were important for survival and reproduction. Such incentive behaviours include eating, drinking and copulation, and are reinforced by so-called 'natural rewards' (for example, food, water, pheromones)[1]. Growing evidence suggests that social interaction itself can act as a natural reward[2]. However, given the diversity of social behaviours (for example, parental investment, mating, cooperation) and the selection pressures that shaped their emergence (reproductive, predation, limited resources)[3], it remains unclear whether evolutionarily conserved neural mechanisms exist to encode social reward.

An important clue comes from studies that have related pair-bonding behaviour in prairie voles (*Microtus ochrogaster*) to elevated expression of oxytocin receptors (OTRs) in the nucleus accumbens (NAc), a key component of the brain's MCL reward circuit[4]. However, the species-specific nature of this mating behaviour and the reported paucity of OTR expression in the NAc of mice[2,5,6] questions the relevance of NAc OTRs to consociate social behaviours. This topic is of particular interest given that polymorphisms in the OTR gene have been associated with autism spectrum disorders, which are characterized by profound social deficits, and may be amenable to treatment with oxytocin (OT)[7].

Mice are social animals: they live in consociate 'demes' consisting of five to ten adult members that share territorial defence[8] and alloparental responsibilities[9], and exhibit several behaviours (for example, vocal communication, imitation, and empathy)[10–12] that are the hallmarks of sociality. As in several other species including humans, OT has been linked to social behaviours in mice[7]. However, OT and OTR knockout mice show a number of related behavioural deficits (such as memory impairment, anxiety, stress, aggressivity)[5] that make it difficult to parse the function of OT as a social reward signal in the central nervous system. To examine the hypothesis that OT signalling in mice is required for the rewarding properties of social interactions, we used a conditioned place preference (CPP) assay that has traditionally been used to study the rewarding properties of drugs of abuse[13] and recently has been expanded to include social reward[14].

Social reward requires oxytocin

Male wild-type mice were conditioned for social CPP (Fig. 1a, b) while receiving intraperitoneal injections of either saline or the OTR antagonist (OTR-A), L-368,899 hydrochloride (5 mg kg^{-1}, twice a day for 2 days). Saline-treated wild-type mice showed a robust place preference for the socially conditioned context, whereas OTR-A treated mice showed no preference (Fig. 1c–e). Neither locomotor activity (Supplementary Fig. 1a–i) nor cocaine CPP (Supplementary Fig. 2a–d) was altered by OTR-A treatment, demonstrating the specificity of the effects of OTR-A for the social domain. Furthermore, OTR-A, but not saline, localized to the NAc using Andalman probes (Fig. 1f and Supplementary Fig. 3a, b) prevented social CPP (Fig. 1g–i), demonstrating that OT action in the NAc is required for consociate social reward.

Given the known species- and sex-specific variation in OTR expression[2,5,15,16], it is notable that no study so far[6,17–19] has determined whether hypothalamic OTergic inputs to the NAc exist in male mice. Here we injected recombinant rabies virus expressing enhanced green fluorescent protein (eGFP) (RBV-eGFP) into the NAc, where it is taken up by presynaptic terminals and retrogradely transported to cell bodies (Supplementary Fig. 4). In a substantial subset of hypothalamic neurons in the paraventricular nucleus (PVN), but not the supraoptic nucleus (SON), robust eGFP expression co-localizes with OT, indicating a direct axonal OTergic projection to the NAc (Supplementary Figs 4 and 5). Furthermore, these results suggest that it is the magnocellular projection from the SON that distinguishes prairie voles[6] from rats[19] and mice. Although they do not rule out an additional contribution of paracrine release, our findings demonstrate a significant synaptic source for OT in the NAc of male mice.

[1]Nancy Pritzker Laboratory, Department of Psychiatry and Behavioral Sciences, Stanford University School of Medicine, 265 Campus Drive, Stanford, California 94305, USA. †Present address: Department of Neuroscience, Johns Hopkins University, 855 North Wolfe Street, Baltimore, Maryland 21205, USA.

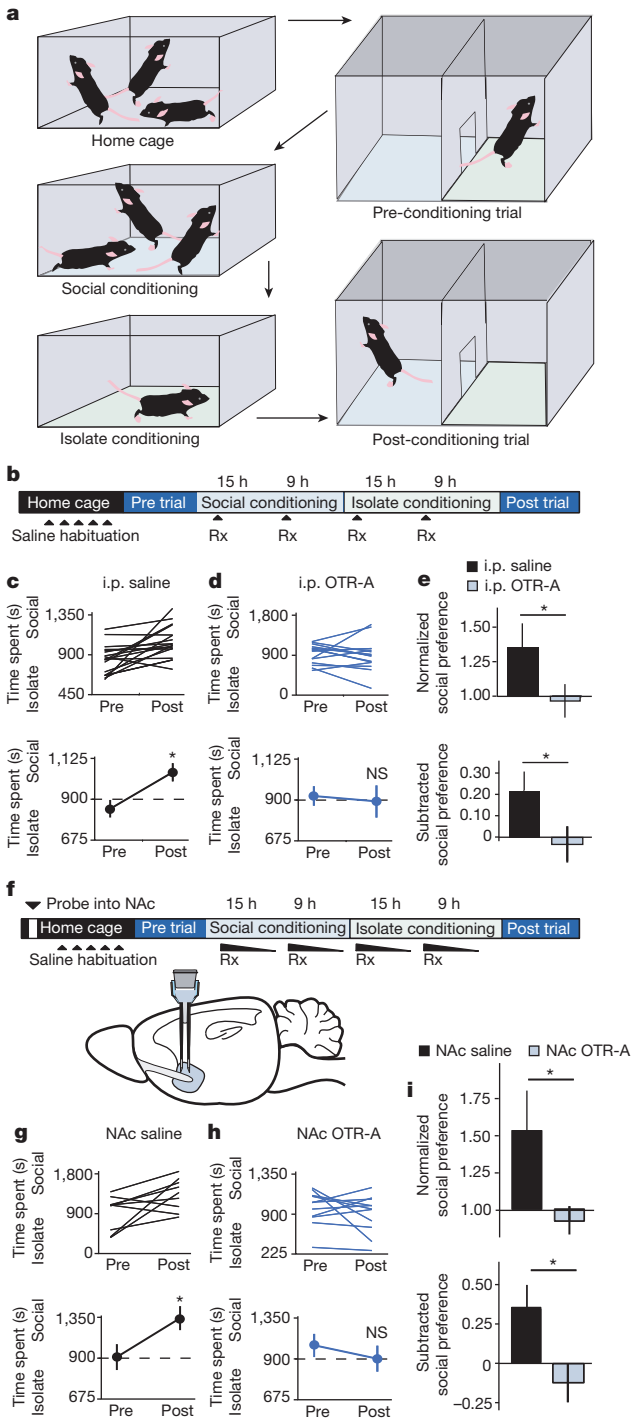

Figure 1 | Oxytocin is required for social CPP. **a–i**, Protocol for social CPP (**a**). Experimental time course of intraperitoneal (i.p.) injections (**b**) and NAc reverse microdialysis (**f**) in social CPP. Individual (top) and average (bottom) responses in animals receiving intraperitoneal (i.p.) (**c**) or NAc (**g**) saline versus animals receiving i.p. (**d**) or NAc (**h**) OTR-A. For both i.p. and NAc delivery routes, saline- but not OTR-A-treated animals spend more time in social bedding cue following conditioning ($n = 18$ i.p. saline, $n = 15$ i.p. OTR-A; $n = 9$ NAc saline and $n = 11$ NAc OTR-A animals). Values below 900 indicate that subjects preferred isolate bedding; values above 900 indicate that subjects preferred social bedding. **e**, **i**, Comparisons between treatment (Rx) groups reveal significantly decreased normalized and subtracted social preference in both i.p. and NAc OTR-A-treated animals. Summary data are presented as mean ± s.e.m. ($^*P < 0.05$, Student's *t*-test). Each arrowhead indicates an application of saline or OTR-A.

Oxytocin induces presynaptic LTD in NAc MSNs

To interrogate directly the synaptic role of OT within the NAc, we recorded excitatory postsynaptic currents (EPSCs) from NAc medium spiny neurons (MSNs) in acute slices. Bath application of OT (1 μM, 10 min) caused a long-term depression (LTD) of EPSCs that was blocked (Fig. 2a–c) but not reversed (Fig. d–f) by the OTR-A L-368,899 hydrochloride (1 μM, continuous or 10 min application respectively). The magnitude of this oxytocin-induced LTD was significantly decreased in slices from socially conditioned versus isolation conditioned animals (Fig. 2g–i), consistent with the hypothesis that social experience elicits or influences the generation of OT-LTD.

To determine whether social experience preferentially influenced OT-LTD in one of the two major components of the basal ganglia circuit, direct (D1-receptor-expressing) versus indirect (D2-receptor-expressing) pathway MSNs[20], targeted recordings were made from NAc slices prepared from bacterial artificial chromosome (BAC) transgenic D1–TdTomato, and D2-eGFP reporter mice[21,22]. Application of OT induced robust LTD (Fig. 2j–l) and isolation conditioning resulted in increased magnitude of OT-LTD (Supplementary Fig. 6) in both D1- and D2-receptor-expressing MSNs, suggesting that these phenomena do not display direct and indirect pathway specificity.

To determine whether the OT-LTD was expressed pre- or postsynaptically, we performed a number of standard electrophysiological synaptic assays. The frequency, but not the amplitude, of miniature EPSCs, was significantly decreased by OT application (Fig. 2m–q). Furthermore, both the paired-pulse ratio (PPR) of EPSCs (50-ms inter-stimulus interval) and the coefficient of variation of the EPSCs increased following OT application (Fig. 2r–t). Together, these findings suggest that OT-LTD results from a decrease in presynaptic neurotransmitter release probability.

Social reward requires presynaptic OTRs in NAc

Anatomical studies have revealed sparse expression of OTRs in mouse NAc[2,5]. Moreover, immunostaining in OTR-Venus reporter mice[23] indicates that the small subset of cells that do express OTRs in the NAc are either inhibitory interneurons or glial cells (Supplementary Fig. 7). To test the hypothesis that OTRs in the NAc are preferentially localized to presynaptic boutons deriving from afferent inputs, we injected TdTomato-expressing RBV (RBV-TdTomato) into the NAc of OTR-Venus reporter mice (Supplementary Fig. 8). Cellular co-localization of TdTomato and Venus was detected in several, but not all, brain regions projecting to the NAc (Supplementary Fig. 8), identifying a number of putative sources of presynaptic OTRs in the NAc.

To extend the anatomical mapping of OTRs to their functional role in social reward *in vivo*, we used conditional OTR knockout mice[24] combined with Cre recombinase (Cre)-expressing RBV or adeno-associated virus (AAV) injected into the NAc, an approach that enabled selective ablation of pre- or postsynaptic NAc OTRs, respectively. Normal social CPP was observed in both sham-injected wild-type and conditional OTR mice (Fig. 3a–d). Injection of the AAV-Cre-eGFP to delete OTRs from cells within the NAc did not affect social CPP in either wild-type or conditional OTR mice (Fig. 3e–h). Consistent with this lack of effect of deleting OTRs from cells within the NAc, OT application did not induce long-lasting changes at inhibitory synapses onto MSNs (Supplementary Fig. 9). In contrast, injection of RBV-Cre-eGFP to delete presynaptic OTRs in the NAc, completely blocked social CPP in conditional OTR knockout mice but had no effect in wild-type mice (Fig. 3i–l). Injection sites and viral expression were confirmed for all animals (Supplementary Figs 10 and 11). Considered together with the pharmacological results showing OTRs within the NAc are required for social CPP (Fig. 1f–i), these results indicate that OTRs on presynaptic boutons within the NAc are required for social reward.

Social CPP and LTD require dorsal raphe inputs and 5HT1B receptors

To determine which of the afferent inputs expressing OTRs identified by RBV-mediated molecular ablation are required for social CPP,

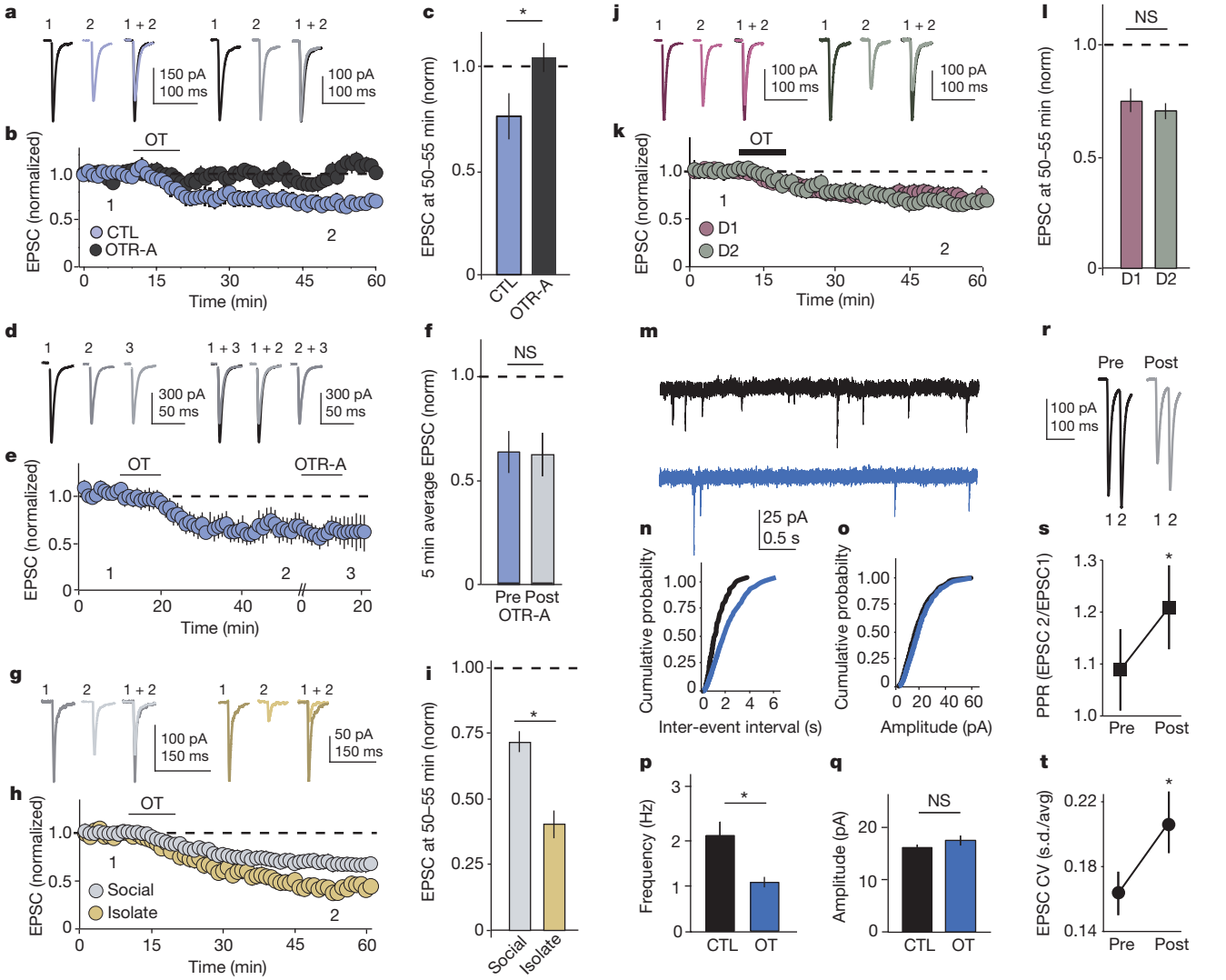

Figure 2 | Oxytocin induces LTD in the NAc. **a–h**, Representative traces (**a**, **d**, **g**, **j**), summary time course (**b**, **e**, **h**, **k**), and average post-treatment magnitude comparisons (**c**, **f**, **i**, **l**) reveal significant EPSC response depression in oxytocin-treated but not OTR-A-pre-incubated cells (**a–c**, $n = 6$ OT (oxytocin), $n = 6$ OT + OTR-A pre-incubation cells). OT-response depression is not reversed by post-induction OTR-A chase (**d–f**, $n = 7$ cells). The magnitude of OT-LTD is significantly increased in cells from isolation versus socially reared animals (**g–i**, isolate, $n = 14$, social $n = 27$ cells). The magnitude of EPSC OT-LTD is not different in D1 versus D2 MSNs (**j-l**, $n = 9$ D1, and $n = 11$ D2 cells). **m–q** Representative miniature EPSC traces (**m**), cumulative probability (**n**, **o**), and average (**p**, **q**) comparisons reveal that miniature EPSC frequency (**n**, **p**), but not amplitude (**o**, **q**), is decreased in OT-treated versus control cells (control, $n = 11$, OT, $n = 11$ cells). **r–t**, Comparisons of representative traces (**r**) and average (**s**) paired-pulse ratios PPR ($n = 6$ cells) as well as average (**t**) coefficient of variance, CV ($n = 32$ cells) reveal significant increases following induction of OT-LTD. Summary data are presented as mean ± s.e.m. (*$P < 0.05$, Student's *t*-test). Numbered traces (1, 2 and 3) were taken at the times indicated by numbers below the graphs.

we next injected AAV-eCre-eGFP into selected brain regions of conditional OTR mice. Deleting OTRs in either the anterior cingulate cortex or the ventral subiculum had no effect on social CPP (Supplementary Fig. 12), whereas AAV-Cre-eGFP injections into the dorsal raphe nucleus of conditional OTR mice, but not wild-type mice, prevented social CPP (Fig. 4a–d). This same manipulation also significantly reduced OT-LTD recorded *ex vivo* (Fig. 4e–g). Together these results provide support for the hypothesis that presynaptic OTRs on dorsal raphe nucleus axon terminals within the NAc are specifically required for social reward.

Since the dorsal raphe nucleus is one of the major sources of serotonin (5-HT) in the brain, we further characterized NAc projection neurons in the dorsal raphe nucleus and found substantial overlap between OTR- and 5-HT-expressing cells (Supplementary Fig. 13), raising the possibility of coordinated activity of these transmitters in the NAc. Given that 5HT1B receptors have been implicated in social behaviours[25,26] and autism[27], and their activation elicits a presynaptic LTD in the striatum[28], we reasoned that OT may induce LTD in the NAc through activation of 5HT1B receptors. Consistent with previous results[28], application of the 5HT1B selective agonist CP-93129 induced robust LTD in NAc MSNs (Fig. 5a–c). Subsequent application of OT caused no further depression (Fig. 5a–c), suggesting that the 5HT1B receptor-induced LTD had occluded OT-LTD. To test whether OT-LTD required release of 5HT within the NAc, we applied the 5HT1B receptor antagonist NAS-181 (20 μM) to NAc slices, a manipulation that largely prevented the LTD normally induced by OT (Fig. 5d–f). In contrast, 5HT1B receptor-induced LTD was readily induced in slices in which OTRs had been pharmacologically blocked (Fig. 5g–i) or molecularly ablated from dorsal raphe nucleus projections (Supplementary Fig. 14). Application of NAS-181 also prevented the decrease in miniature EPSC frequency normally elicited by OT (Fig. 5j–n), but had no effect on its own (Supplementary Fig. 15).

Together these results support the hypothesis that activation of OTRs on the terminals of dorsal raphe nucleus axons within the NAc leads to a 5HT1B receptor-dependent form of LTD (Supplementary Fig. 16) and that this synaptic modulation is necessary for social reward, as measured by social CPP. A strong prediction of this hypothesis is that

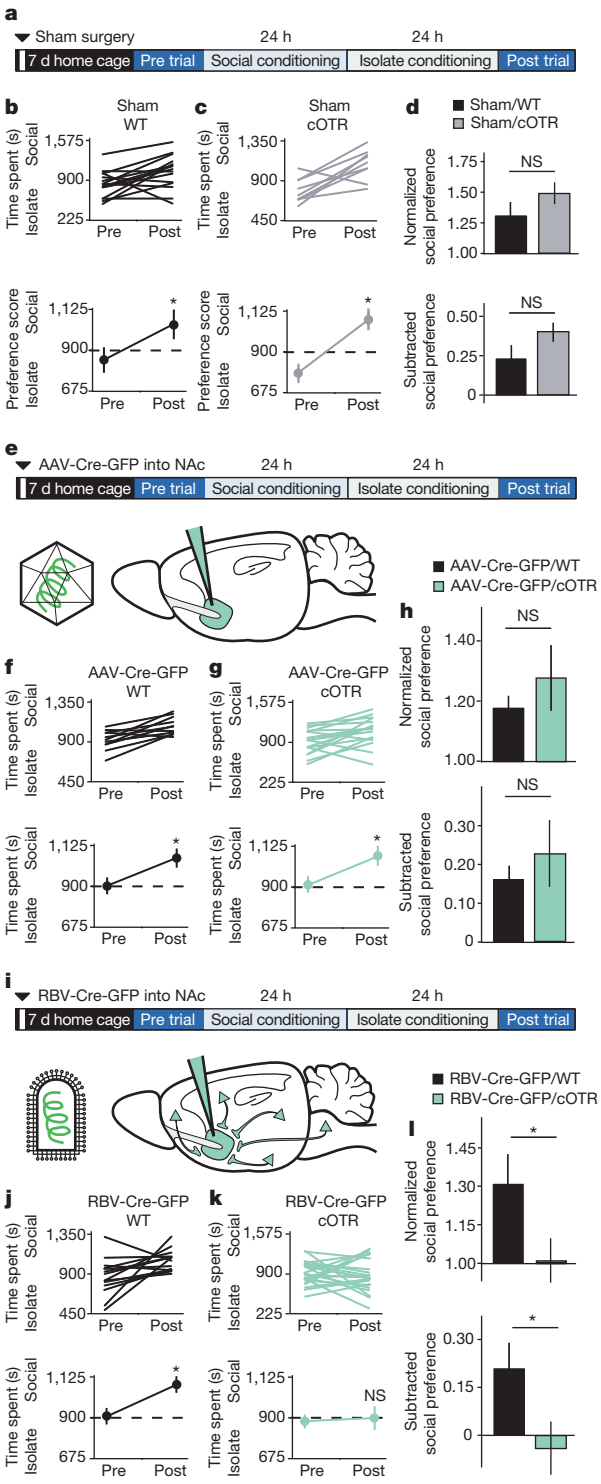

Figure 3 | Presynaptic OTRs are required for social CPP. a–l, Experimental time course for sham (**a**), NAc AAV-Cre-eGFP injection showing AAV particle and spread of Cre-eGFP from injection site (**e**), and NAc RBV-Cre-eGFP injection showing RBV particle and spread of Cre-eGFP from injection site (**i**). Individual (top) and average (bottom) responses in wild-type (WT) (**b**, **f**, **j**), versus conditional OTR (cOTR) (**c**, **g**, **k**) animals receiving sham (**b**, **c**), NAc AAV-Cre-eGFP (**f**, **g**) or NAc-RbV-Cre-eGFP (**j**, **k**). WT animals, as well as sham and NAc AAV-Cre-eGFP-injected cOTR animals, but not cOTR animals injected with NAc RBV-Cre-eGFP, spend more time in the social bedding cue following conditioning (sham WT, $n = 15$, cOTR, $n = 8$; NAc AAV-Cre-eGFP WT, $n = 15$, cOTR, $n = 19$; NAc RBV-Cre-eGFP WT, $n = 14$, cOTR, $n = 22$ animals). **d**, **h**, **l**, Comparisons between WT and cOTR animals reveal normal social CPP in sham and NAc AAV-Cre-eGFP-injected animals, whereas in NAc RBV-Cre-eGFP-injected animals social CPP is significantly decreased in cOTR versus WT controls. Summary data are presented as mean ± s.e.m. (*$P < 0.05$, Student's *t*-test).

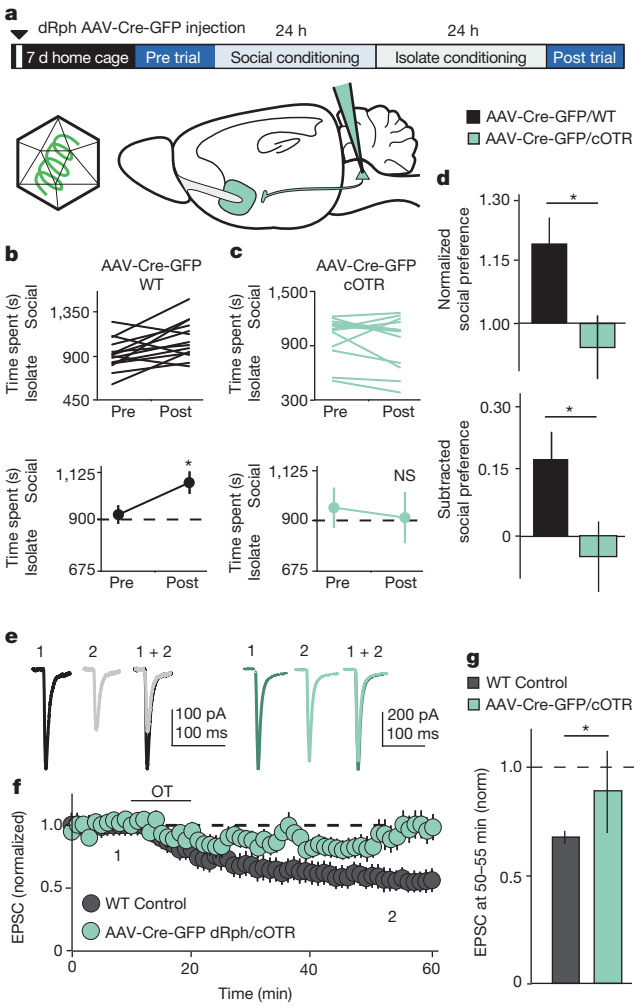

Figure 4 | NAc OTRs in presynaptic terminals originating from the dorsal raphe nucleus are required for social CPP and OT-LTD. a, Experimental time course of dorsal raphe nucleus (dRph) AAV-Cre-eGFP injections in social CPP. **b**, **c** Individual (top) and average (bottom) comparisons reveal that dRph AAV-Cre-eGFP-injected WT (**b**), but not cOTR (**c**) animals spend significantly more time in the social bedding cue following conditioning (WT, $n = 14$, cOTR, $n = 10$ animals). **d**, Comparisons between dRph AAV-Cre-eGFP-injected groups reveal significantly decreased social CPP in cOTR animals compared to WT controls. **e–g**, Representative traces (**e**), summary time course (**f**) and average post-treatment magnitude comparisons (**g**) reveal absence of OT-LTD in EPSCs recorded from dRph AAV-Cre-eGFP-injected cOTR knockout versus pooled WT control animals (dRph AAV-Cre-eGFP-injected cOTR, $n = 6$ cells; pooled WT control, $n = 30$ cells). Summary data are presented as mean ± s.e.m. (*$P < 0.05$, Student's *t*-test).

blockade of 5HT1B receptors within the NAc should prevent social CPP. Consistent with this prediction, NAS-181, but not saline, infusions into the NAc during conditioning (Fig. 6a) prevented the occurrence of social CPP (Fig. 6b–d).

Concluding remarks

We have demonstrated that the coordinated activity of OT and 5-HT is required for the reward associated with social interactions and modifies MCL circuit properties by generating LTD of excitatory synapses onto MSNs in the NAc. Moreover, our findings specifically implicate OT-mediated 5-HT release in the NAc in the regulation of social reward. Since OT-LTD occurs in both D1- and D2-receptor-expressing MSN subtypes, as does 5HT1B-LTD[28], these results suggest that social reward is not expressly governed by the dichotomies proposed by prevailing models of striatal function[20]. Indeed, the two-pathway framework for striatal function is almost certainly oversimplified[29–32] and computational

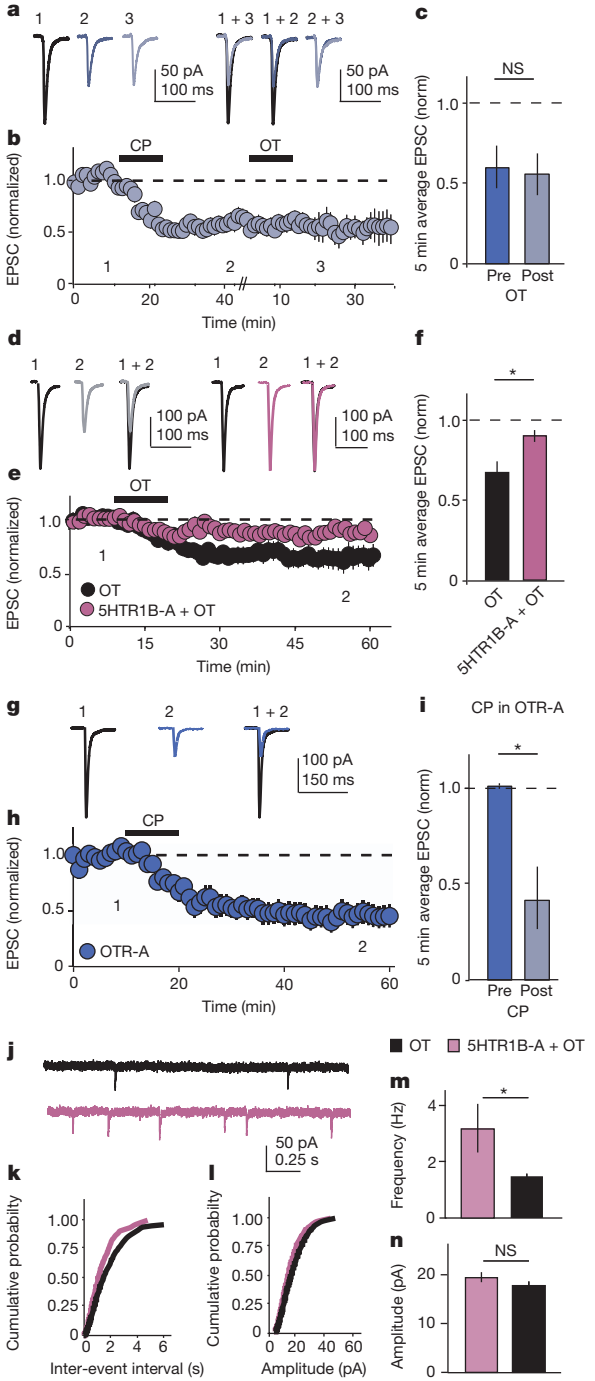

Figure 5 | OT-LTD in NAc requires 5HT1B receptors. **a–i**, Representative traces (**a**, **d**, **g**), summary time course (**b**, **e**, **h**) and average post-treatment magnitude comparisons (**c**, **f**, **i**) reveal that EPSC depression in cells treated with 5HTR1B agonist (CP-93129 dihydrochloride) is not augmented by subsequent application of OT (**a–c**, $n = 5$ cells); OT-LTD is significantly reduced in cells pre-treated with the 5HTR1b-antagonist (NAS-181) (**d–f**, control, $n = 7$, 5HTR1B antagonist, $n = 7$ cells); 5HTR1B-mediated LTD induced by application of CP-93129 is not affected by pharmacological blockade of OTRs (**g–i**, $n = 5$ cells). **j–n** Representative miniature EPSC traces (**j**), cumulative probability (**k**, **l**), and average **(m, n)** comparisons reveal miniature EPSC frequency (**k**, **m**), but not amplitude (**l**, **n**), is decreased in OT-treated cells versus cells treated with OT in the presence of NAS-181 (OT, $n = 17$, OT + 5HTR1b-A, $n = 17$ cells). Summary data are presented as mean ± s.e.m. (*$P < 0.05$, Student's *t*-test).

modelling studies have proposed that reinforcement learning engages multiple neuromodulatory reward circuits in parallel[33]. Furthermore, 5-HT and dopamine systems may represent reward in fundamentally

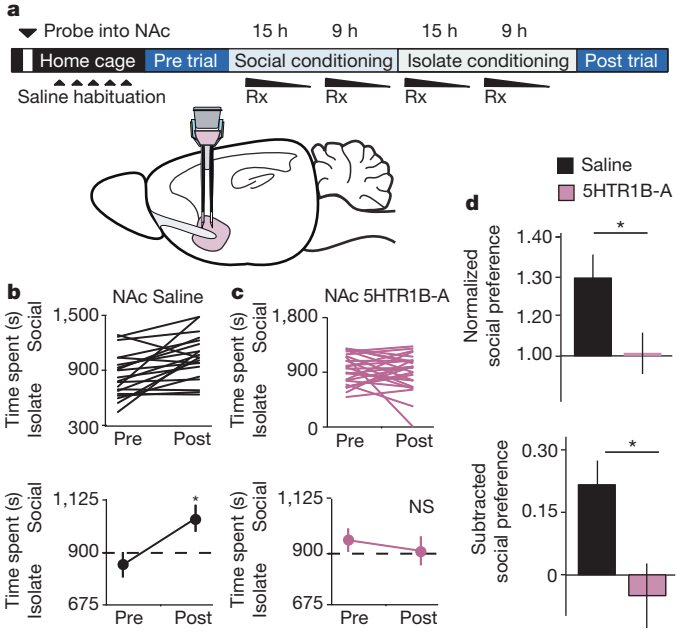

Figure 6 | Social CPP requires NAc 5HT1B receptors. **a**, Experimental time course of NAc reverse microdialysis. **b**, **c**, Individual (top) and average (bottom) responses in animals receiving NAc saline (**b**) versus 5HTR1B antagonist (5HTR1B-A) (**c**). Saline-treated animals, but not 5HTR1B-A-treated animals, spend more time in social bedding cue following conditioning (NAc saline, $n = 20$, NAc 5HTR1B-A, $n = 26$ animals). **d**, Comparisons between treatment groups reveal significantly decreased normalized and subtracted social preference in NAc 5HTR1B-A-treated animals compared to saline controls. Summary data are presented as mean ± s.e.m. (*$P < 0.05$, Student's *t*-test).

different ways[34–36]. Future studies examining the interplay between dopamine and 5-HT in the regulation of social reward will therefore be informative.

In light of estimates that the shift to social living preceded the emergence of pair-living by 35 million years[3], we suggest that the NAc-dependent social reward mechanisms described here are the predecessors of evolutionary specializations seen in prairie voles[2,5,6]. These mechanisms utilize presynaptically localized OTRs, which couple to G-proteins[5], and thus may have been overlooked by previous studies that relied on receptor autoradiography and transcript tagging to conclude that OTRs do not exist in the NAc of consociate species like mice[2,6]. Moreover, as it is these antecedent social behaviours that are disrupted in neuropsychiatric diseases such as autism[37], the elucidation of the neural mechanisms mediating social reward is a critical step towards the development of rational, mechanism-based treatments for brain disorders that involve dysfunction in social behaviours.

METHODS SUMMARY

All procedures were conducted in accordance with the animal care standards set forth by the National Institutes of Health and were approved by Stanford University's Administrative Panel on Laboratory Animal Care. Male young adult mice (4 to 6 weeks of age) on a C57BL/6 background were used for all studies.

Full Methods and any associated references are available in the online version of the paper.

Received 26 November 2012; accepted 1 August 2013.

1. Kelley, A. E. & Berridge, K. C. The neuroscience of natural rewards: relevance to addictive drugs. *J. Neurosci.* **22,** 3306–3311 (2002).
2. Insel, T. R. Is social attachment an addictive disorder? *Physiol. Behav.* **79,** 351–357 (2003).
3. Shultz, S., Opie, C. & Atkinson, Q. D. Stepwise evolution of stable sociality in primates. *Nature* **479,** 219–222 (2011).
4. Young, L. J. & Wang, Z. The neurobiology of pair bonding. *Nature Neurosci.* **7,** 1048–1054 (2004).
5. Lee, H.-J., Macbeth, A. H., Pagani, J. H. & Young, W. S. Oxytocin: the great facilitator of life. *Prog. Neurobiol.* **88,** 127–151 (2009).

6. Ross, H. E. *et al.* Characterization of the oxytocin system regulating affliative behavior in female prairie voles. *Neurosci.* **162,** 892–903 (2009).
7. Yamasue, H. *et al.* Integrative approaches utilizing oxytocin to enhance prosocial behavior: from animal and human social behavior to autistic social dysfunction. *J. Neuroscience* **32,** 14109–14117 (2012).
8. Anderson, P. K. & Hill, J. *Mus musculus*: experimental induction of territory formation. *Science* **148,** 1753–1755 (1965).
9. Riedman, M. L. The evolution of alloparental care and adoption in mammals and birds. *Q. Rev. Biol.* **57,** 405–435 (1982).
10. Holy, T. E. & Guo, Z. Ultrasonic songs of male mice. *PLoS Biol.* **3,** e386 (2005).
11. Panksepp, J. Behavior. Empathy and the laws of affect. *Science* **334,** 1358–1359 (2011).
12. Hodgson, S. R., Hofford, R. S., Roberts, K. W., Wellman, P. J. & Eitan, S. Socially induced morphine pseudosensitization in adolescent mice. *Behav. Pharmacol.* **21,** 112–120 (2010).
13. Tzschentke, T. M. Measuring reward with the conditioned place preference (CPP) paradigm: update of the last decade. *Addict. Biol.* **12,** 227–462 (2007).
14. Panksepp, J. B. & Lahvis, G. P. Social reward among juvenile mice. *Genes Brain Behav.* **6,** 661–671 (2007).
15. Rosen, G. J., de Vries, G. J., Goldman, S. L., Goldman, B. D. & Forger, N. G. Distribution of oxytocin in the brain of a eusocial rodent. *Neuroscience* **155,** 809–817 (2008).
16. Hermes, M. L., Buijs, R. M., Masson-Pévet, M. & Pévet, P. Oxytocinergic innervation of the brain of the garden dormouse (*Eliomys quercinus* L.). *J. Comp. Neurol.* **273,** 252–262 (1988).
17. Phillipson, O. T. & Griffiths, A. C. The topographic order of inputs to nucleus accumbens in the rat. *Neuroscience.* **16,** 275–296 (1985).
18. Brog, J. S., Ongse, A. S., Deutch, A. Y. & Zahm, D. S. The patterns of afferent innervation of the core and shell in the ''accumbens'' part of the rat ventral striatum: immunohistochemical detection of retrogradely transported fluoro-gold. *J. Comp. Neurol.* **278,** 255–278 (1993).
19. Knobloch, H. S. *et al.* Evoked axonal oxytocin release in the central amygdala attenuates fear response. *Neuron* **73,** 553–566 (2012).
20. Lobo, M. K. & Nestler, E. J. The striatal balancing act in drug addiction: distinct roles of direct and indirect pathway medium spiny neurons. *Front. Neuroanat.* **5,** 41 (2011).
21. Shuen, J. A., Chen, M., Gloss, B. & Calakos, N. Drd1a-tdTomato BAC transgenic mice for simultaneous visualization of medium spiny neurons in the direct and indirect pathways of the basal ganglia. *J. Neurosci.* **28,** 2681–2685 (2008).
22. Gong, S. *et al.* A gene expression atlas of the central nervous system based on bacterial artificial chromosomes. *Nature* **425,** 917–925 (2003).
23. Yoshida, M. *et al.* Evidence that oxytocin exerts anxiolytic effects via oxytocin receptor expressed in serotonergic neurons in mice. *J. Neurosci.* **29,** 2259–2271 (2009).
24. Lee, H.-J., Caldwell, H. K., Macbeth, A. H., Tolu, S. G. & Young, W. S. A conditional knockout mouse line of the oxytocin receptor. *Endocrinology* **149,** 3256–3263 (2008).
25. Brunner, D., Buhot, M. C., Hen, R. & Hofer, M. Anxiety, motor activation, and maternal-infant interactions in 5HT1B knockout mice. *Behav. Neurosci.* **113,** 587–601 (1999).
26. Furay, A. R., McDevitt, R. A., Miczek, K. A. & Neumaier, J. F. 5–HT1B mRNA expression after chronic social stress. *Behav. Brain Res.* **224,** 350–357 (2011).
27. Orabona, G. M. *et al.* HTR1B and HTR2C in autism spectrum disorders in Brazilian families. *Brain Res.* 1250**,** 14–19 (2009); erratum **1264,** 127 (2009).
28. Mathur, B. N., Capik, N. A., Alvarez, V. A. & Lovinger, D. M. Serotonin induces long-term depression at corticostriatal synapses. *J. Neurosci.* **31,** 7402–7411 (2011).
29. Cui, G. *et al.* Concurrent activation of striatal direct and indirect pathways during action initiation. *Nature* **494,** 238–242 (2013).
30. Capper-Loup, C., Canales, J. J., Kadaba, N. & Graybiel, A. M. Concurrent activation of dopamine D1 and D2 receptors is required to evoke neural and behavioral phenotypes of cocaine sensitization. *J. Neurosci.* **22,** 6218–6227 (2002).
31. Nambu, A. Seven problems on the basal ganglia. *Curr. Opin. Neurobiol.* **18,** 595–604 (2008).
32. Perreault, M. L., Hasbi, A., O'Dowd, B. F. & George, S. R. The dopamine d1-d2 receptor heteromer in striatal medium spiny neurons: evidence for a third distinct neuronal pathway in Basal Ganglia. *Front. Neuroanat.* **5,** 31 (2011).
33. Doya, K. Metalearning and neuromodulation. *Neural Netw.* **15,** 495–506 (2002).
34. Nakamura, K., Matsumoto, M. & Hikosaka, O. Reward-dependent modulation of neuronal activity in the primate dorsal raphe nucleus. *J. Neurosci.* **28,** 5331–5343 (2008).
35. Tanaka, S. C. *et al.* Prediction of immediate and future rewards differentially recruits cortico-basal ganglia loops. *Nature Neurosci.* **7,** 887–893 (2004).
36. Boureau, Y.-L. & Dayan, P. Opponency revisited: competition and cooperation between dopamine and serotonin. *Neuropsychopharmacology* **36,** 74–97 (2011).
37. Silverman, J. L., Yang, M., Lord, C. & Crawley, J. N. Behavioural phenotyping assays for mouse models of autism. *Nature Rev. Neurosci.* **11,** 490–502 (2010).

Supplementary Information is available in the online version of the paper.

Acknowledgements We thank members of the Malenka laboratory for comments; A. Andalman, W. Xu, B.K. Lim and T. Sudhof for technical advice; and the SIM1 Animal Care facility for husbandry support. The OT-neurophysin antibody was a gift of H. Gainer. OTR-Venus reporter mice were a gift of L. J. Young. D1-TdTomato BAC transgenic mice were provided by N. Calakos. The rabies virus complementary DNA plasmid and viral component-expressing plasmids were gifts from K. Conzelmann and I. Wickersham. HHK-B19G cells were a gift from E. Callaway. AAVs were produced by the Stanford NGVVC (supported by National Institutes of Health grant NIH NS069375). The AAV-DJ helper plasmid was a gift from M. Kay. This work was supported by funding from the Simons Foundation Autism Research Initiative (R.C.M.), N.I.H. (R.C.M.), and a Berry Foundation Postdoctoral Fellowship (G.D.)

Author Contributions G.D. and R.C.M. designed the study, interpreted results and wrote the paper. G.D. performed behavioural experiments, electrophysiology, and confocal microscopy. G.D., A.D. and K.W.H. performed stereotaxic injections and immunohistochemistry. K.W.H. generated RBV viruses. All authors edited the paper.

Author Information Reprints and permissions information is available at www.nature.com/reprints. The authors declare no competing financial interests. Readers are welcome to comment on the online version of the paper. Correspondence and requests for materials should be addressed to R.C.M. (malenka@stanford.edu).

METHODS

Animals. Male young adult (4 to 6 weeks of age) C57BL/6 (Charles River), DRD1A–TdTomato BAC transgenic[21] (D1-TdTomato, gift of N. Calakos), DRD2–eGFP BAC transgenic[22] (D2-eGFP), Oxtrtm1.1Wsy homozygous[24] (conditional OTR knockout, Jackson Laboratory), or OTR Venus Neo/+[23] (heterozygous OTR-Venus reporter, gift of L. J. Young) mice backcrossed to C57BL/6 were used for all experiments. All procedures complied with the animal care standards set forth by the National Institutes of Health and were approved by Stanford University's Administrative Panel on Laboratory Animal Care. All animals were maintained on a 12 h–12 h light–dark cycle. Experimenters were blind to the treatment condition when subjective criteria were used as a component of data analysis, and control and test conditions were interleaved for all experiments.

Behavioural assays. The protocol for social conditioned place preference (social CPP) was shortened to 2 days of conditioning (Fig. 1a) from 10 days of conditioning[14,38]. Animals were weaned (or delivered from Charles River) at 3 weeks of age into 'home' cages containing 3 to 5 cage-mates, and housed on corncob bedding (Bed-O'Cobs, 0.125 inches, PharmaServ). One to two weeks later, animals were subjected to experimental manipulations and returned to their home cage (all cage-mates were of the same genotype and received the same experimental manipulation). Animals were then placed in open field activity chamber (ENV-510, Med Associates) equipped with infrared beams and a software interface (Activity Monitor, Med Associates) that monitors the position of the mouse. The apparatus was divided into two equally sized zones using a clear plastic wall, with a 5-cm diameter circular opening at the base; each zone contained one type of novel bedding (Alpha-Dri, PharmaServ, Alpha Chip, PharmaServ; Bed-O'Cobs, 0.25 inches, PharmaServ; or Kaytee Soft Granule, Petco). The amount of time spent freely exploring each zone was recorded during 30-min test sessions. After an initial test (pre-conditioning trial) to establish baseline preference for the two sets of bedding cues, mice were assigned to receive social conditioning (with cage-mates) for 24 h on one type of bedding, followed by 24h on the isolate bedding cue (without cage-mates) on the other type of bedding. Bedding assignments (social versus isolate) were counterbalanced for an unbiased design. Twenty-four hours later, animals received a 30-min post-conditioning trial to establish preference for the two conditioned cues. Animals were excluded (pre-established criteria) if they exhibited a pre-conditioning preference score of >1.5 or <0.5 (for an unbiased procedure); pre-conditioning versus post-conditioning social preference scores were considered significant if paired student's *t*-test P values were <0.05. Comparisons between experimental conditions were made using both normalized social preference scores (time spent in social zone; post-trial divided by pre-trial), and subtracted social preference scores (time spent in social zone; post-trial minus pre-trial); these were considered significant if unpaired student's *t*-test (two conditions), or analysis of variance (ANOVA) (three conditions, Supplementary Fig. 12) *P* values were <0.05.

For cocaine-conditioned place preference (cocaine CPP), the apparatus was divided into two equally sized zones using plastic floor tiles with distinct visual and tactile cues (grey and smooth, or white and rough). After 5 days of saline injections twice a day for habituation in the home cage, the amount of time spent freely exploring each zone was recorded during 30-min test sessions. After an initial test to establish baseline preference for the two sets of cues, mice in each of the two treatment groups (intraperitoneal saline or intraperitoneal OTR-A) were randomly assigned in a counterbalanced fashion to receive cocaine (20 mg kg^{-1}) or saline in the presence of one set of cues (that is, an unbiased design). The second conditioning session was conducted 24 h later in the presence of the other set of cues. The post-conditioning test session was conducted 24 h after the second conditioning session to determine time spent in the presence of the cocaine versus saline associated cue. Isolation and socially housed animals were not different in terms of cocaine CPP so they were pooled for further analysis. Pre-conditioning, post-conditioning, subtracted, and normalized cocaine preference scores were calculated as for social CPP.

Andalman probes. Modified Andalman probes were constructed as described previously[39] (Supplementary Fig. 3). In brief, probes consisted of a reservoir (Polypropylene Luer Hub) attached to a double cannula guide (C235gs, 26GA, C/C distance 2 mm, 5 mm pedestal, cut 4 mm below pedestal, custom specified for mouse bilateral NAc coordinates, Plastics One). Polyimide tubing (40 American Wire Gauge, 0.0031 inches internal diameter, 0.0046 inches outside diameter, 0.00075 inches Wall, Small Parts) was threaded through the stainless steel tubing of the cannula guide on one end, and out of a hole drilled into the luer hub to act as a flush outlet (outflow tube) on the other end. The dialysis membrane (Spectra/Por, 13-kD molecular weight cut-off, Spectrum Laboratories) was then threaded over the outflow tube and through the cannula guide; ends were cut such that ~500 μm of dialysis membrane was exposed below the cannula guide and above the sealed end. Junctions were sealed with bio-compatible epoxies (Epo-Tek 730, Epo-Tek 301, Epoxy Technologies). In this design, a pharmacological agent could be intracranially delivered rapidly, continually and concurrently to all members of the social group, without anaesthesia.

Once male mice reached age postnatal day 35 to 40, probes were implanted into the NAc of male mice following bilateral craniotomy (bregma 1.54 mm; lateral 1.0 mm) and attached to the skull using dental acrylic. Previous reports indicate that for complete pharmacological effect, drug concentration in the reservoir must be ~500 times the dose used for direct injections[39,40], thus OTR and 5HTR1B antagonists were applied at 10 mM (L-368,899) and 85 mM (NAS-181) concentrations in a volume of 25 μl saline. Probe placement and competency was verified by post-hoc application of concentrated Fluorescein sodium salt (Sigma-Aldrich) to reservoir before intracardial PFA perfusion and histology (Supplementary Fig. 3).

Virus generation. Rabies virus (RBV) was generated from a full-length complementary DNA plasmid containing all components of RBV (SAD L16; gift from K.-K. Conzelmann)[41]. We replaced the rabies virus glycoprotein with eGFP (RBV-eGFP), TdTomato (RBV-TdTomato) or Cre-eGFP to generate RBV-expressing Cre-eGFP (RBV-Cre-eGFP), eGFP (RBV-eGFP) or TdTomato (RBV-TdTomato). To rescue RBV from this cDNA we used a modified version of a published protocol[41,42]. In brief, HEK293T cells were transfected with a total of 6 plasmids; 4 plasmids expressing the RBV components pTIT-N, pTIT-P, pTIT-G and pTIT-L; one plasmid expressing T7 RNA polymerase (pCAGGS-T7), and the aforementioned glycoprotein-deleted RBV cDNA plasmid expressing Cre-eGFP, eGFP or TdTomato. For the amplification of RBV, the media bathing these HEK293T (ATCC) cells was collected 3 to 4 days post transfection and moved to baby hamster kidney (BHK) cells stably expressing RBV glycoprotein (BHK-B19G)[43]. After 3 days, the media from BHK-B19G cells were collected, centrifuged for 5 min at 3,000*g* to remove cell debris, and concentrated by ultracentrifugation (55,000*g* for 2 h). Pellets were suspended in Dulbecco's PBS, aliquoted and stored at −80 °C. The titre of concentrated RBV was measured by infecting HEK293 cell and monitoring fluorescence. Plasmids expressing the RBV components were gifts from K.-K. Conzelmann and I. Wickersham. BHK cells stably expressing B19G were a gift from E. Callaway.

The adeno-associated viruses (AAVs) used in this study were produced by the Stanford Neuroscience Gene Vector and Virus Core. In brief, AAV-DJ[44] was produced by transfection of AAV 293 cells (Agilent) with three plasmids: an AAV vector expressing Cre-eGFP, AAV helper plasmid (pHELPER, Agilent), and AAV rep-cap helper plasmid (pRC-DJ, gift from M. Kay). At 72 h after transfection, the cells were collected and lysed by a freeze-and-thaw procedure. Viral particles were then purified by an iodixanol step gradient ultracentrifugation method. The iodixanol was diluted and the AAV was concentrated using a 100-kDa molecular weight cut-off ultrafiltration device. The genomic titre was determined by quantitative PCR.

Stereotaxic injections. Stereotaxic injection of viruses into NAc was performed under general ketamine–medetomidine anaesthesia using a stereotaxic instrument (David Kopf). A small volume (~1 μl) of concentrated virus solution was injected bilaterally into NAc core (bregma 1.54 mm; lateral 1.0 mm; ventral 4.0 mm), unilaterally into the dorsal raphe nucleus (bregma −3.3 mm; lateral 0.0 mm; ventral 3.35 mm), bilaterally into the ventral subiculum (bregma −2.95 mm; lateral 3.1 mm; ventral 4.35 mm), or bilaterally anterior cingulate (bregma 1.0 mm; lateral 0.3 mm; ventral 1.25 mm) at a slow rate (100 nl per min) using a syringe pump (Harvard Apparatus). The injection needle was withdrawn 5 min after the end of the infusion. Animals were tested 7 days after AAV or RBV injections. Injection sites and viral infectivity were confirmed in all animals post-hoc by preparing sections (50 μm) containing the relevant brain region (Supplementary Fig. 10).

Immunohistochemistry. Immunohistochemistry and confocal microscopy were performed as described previously[45]. In brief, after intracardial perfusion with 4% paraformaldehyde in PBS (pH 7.4), the brains were post fixed overnight in this same solution and the following day 50 μM coronal, sagittal or horizontal sections were prepared. Primary antibodies were used at the following concentrations: mouse anti-oxytocin-neurophysin (1:50; gift of H. Gainer[46,47]); rat anti-green fluorescent protein (GFP, 1:1000; Nacalai); rabbit anti-parvalbumin (1:750; Swant); rabbit anti-neuronal nitric oxide synthase (1:100; BD Transduction Laboratories); rabbit anti-glial fibrillary protein (1:80; Sigma-Aldrich); rabbit anti-choline acetyltransferase (1:100; Millipore); rabbit anti-dopamine receptor protein (1:100, Millipore); sheep anti-tryptophan hydroxylase (1:100 Millipore) diluted in a solution containing 1% horse serum, 0.2% BSA and 0.5% Triton X-100 in PBS. After overnight incubation in primary antibody at room temperature (20–22 °C) with slow agitation, slices were washed four times in PBS and then incubated with appropriate secondary antibody diluted at 1:750 for 2 h in PBS containing 0.5% Triton X-100. Subsequently, slices were washed 5 times and mounted using Vectashield mounting medium (Vector Laboratories). To identify cells expressing GFP or TdTomato due to the injection of RBV-eGFP or RBV-TdTomato into the NAc, raw fluorescence was visualized. Image acquisition was performed with a confocal microscope (Zeiss LSM510) using a 10×/0.30 Plan Neofluar and a 40×/1.3 Oil DIC Plan Apochromat objective. Confocal images were examined using the Zeiss LSM Image Browser software.

Electrophysiology. Parasagittal slices (250 μm) containing the NAc core were prepared from C57BL/6 and D1-TdTomato/D2-eGFP BAC transgenic mice on a C57BL/6 background using standard procedures. In brief, after mice were anaesthetized with isoflurane and decapitated, brains were quickly removed and placed in ice-cold low sodium, high sucrose dissecting solution. Slices were cut by adhering the two sagittal hemispheres brain containing the NAc core to the stage of a Leica vibroslicer. Slices were allowed to recover for a minimum of 60 min in a submerged holding chamber (~25 °C) containing artificial cerebrospinal fluid (ACSF) consisting of 119 mM NaCl, 2.5 mM KCl, 2.5 mM $CaCl_2$, 1.3 mM $MgSO_4$, 1 mM NaH_2PO_4, 11 mM glucose and 26.2 mM $NaHCO_3$. Slices were then removed from the holding chamber and placed in the recording chamber where they were continuously perfused with oxygenated (95% O_2, 5% CO_2) ACSF at a rate of 2 ml per min at 26 ± 2 °C. For EPSC recordings, bicuculline (20 μM) was added to the ACSF to block $GABA_A$ (γ-aminobutyric acid type A)-receptor–mediated inhibitory synaptic currents. For inhibitory postsynaptic current (IPSC) recordings, dl-2-amino-5-phosphonovalerate (dAPV, 10 μM) and 2,3-Dioxo-6-nitro-1,2,3,4-tetrahydrobenzo[f]quinoxaline-7-sulfonamide (NBQX, 5 μM) dissolved in DMSO were added to block NMDA and AMPA receptors, respectively. Whole-cell voltage-clamp recordings from MSNs were obtained under visual control using a 40× objective. The NAc core was identified by the presence of the anterior commissure. D1 and D2 MSNs in the NAc core were identified by the presence of TdTomato and eGFP, respectively, which were excited with ulraviolet light using bandpass filters (HQ545/30× EX (excitation) for TdTomato; HQ470/40× EX for eGFP). Recordings were made with electrodes (3.5–6.5 MΩ) filled with 115 mM $CsMeSO_4$, 20 mM CsCl, 10 mM HEPES, 0.6 mM EGTA, 2.5 mM MgCl, 10 mM Na-phosphocreatine, 4 mM Na-ATP, 0.3 mM Na-GTP, and 1 mM QX-314. Excitatory and inhibitory afferents were stimulated with a bipolar nichrome wire electrode placed at the border between the NAc core and cortex dorsal to the anterior commissure. Recordings were performed using a Multiclamp 700B (Molecular Devices), filtered at 2 kHz and digitized at 10 kHz. EPSCs were evoked at a frequency of 0.1 Hz while MSNs were voltage-clamped at −70 mV. Data acquisition and analysis were performed on-line using custom Igor Pro software. Input resistance and access resistance were monitored continuously throughout each experiment; experiments were terminated if these changed by >15%.

Summary LTD graphs were generated by averaging the peak amplitudes of individual EPSCs in 1-min bins (six consecutive sweeps) and normalizing these to the mean value of EPSCs collected during the 10 min baseline immediately before the LTD-induction protocol. Individual experiments were then averaged together. Oxytocin (Tocris Biosciences, 1 μM, 10 min) was applied via the bath following the collection of baseline for induction of OT-LTD. For experiments examining the blockade of OT-LTD, slices were pre-incubated in antagonist (OTR-A, 1 μM L-368,899 hydrochloride or 5HTR1B-A, 20 μM NAS-181; Tocris Biosciences) for at least 30 min before recording. For experiments examining the reversal of OT-LTD, 30 to 40 min post induction, OTR-A was bath applied for 10 min. After the collection of stable baseline EPSCs, 5HT1B-LTD was induced by 10-min bath application of 2 μM CP-93129 dihydrochloride (Tocris Biosciences) as described previously[28]. For experiments examining the occlusion of OT-LTD, after stabilization of 5HT1B-LTD (at 30 to 40 min post induction), 1 μM oxytocin was applied via the bath for 10 min. Miniature EPSCs were collected at a holding potential of −70 mV in the presence of TTX (0.5 μM). Two minutes after break-in (sweep number 5, 30-s sweeps), 30-s blocks of events (total of 200 events per cell) were acquired and analysed using Mini-analysis software (Synaptosoft) with threshold parameters set at 5 pA amplitude and <3 ms rise time. All events included in the final data analysis were confirmed to be miniature EPSCs by visual examination, based on their rapid rise time and shape. Slices were incubated in the appropriate drug (dissolved in ACSF-bicuculline) for 10 min before recording, and cross-cell comparisons were made. Paired-pulse ratios (PPRs) were acquired by applying a second afferent stimulus of equal intensity, 50 ms after the first stimulus, and then calculating the ratio of EPSC2/EPSC1. Coefficient of variance was calculated from the standard deviation divided by the average (STDEV/AVG) of 10-min blocks (minutes 0–10, pre trial; minutes 40–50, post trial). Comparisons between different experimental manipulations were made using a two-tailed, Students *t*-test (paired or unpaired, as appropriate) with $P < 0.05$ considered to be significant. All statements in the text regarding differences between grouped data indicate that statistical significance was achieved, assuming normal distribution and equal variance. Sample size was estimated based on published literature[14,28]. All values are reported as mean ± s.e.m.

38. Panksepp, J. B. *et al.* Affiliative behavior, ultrasonic communication and social reward are influenced by genetic variation in adolescent mice. *PLoS ONE* **2,** e351 (2007).
39. Aronov, D., Andalman, A. S. & Fee, M. S. A specialized forebrain circuit for vocal babbling in the juvenile songbird. *Science* **320,** 630–634 (2008).
40. Andalman, A. S. & Fee, M. S. A basal ganglia-forebrain circuit in the songbird biases motor output to avoid vocal errors. *Proc. Natl Acad. Sci. USA* **106,** 12518–12523 (2009).
41. Mebatsion, T., Konig, M. & Conzelmann, K. K. Budding of rabies virus particles in the absence of the spike glycoprotein. *Cell* **84,** 941–951 (1996).
42. Wickersham, I. R., Sullivan, H. A. & Seung, H. S. Production of glycoprotein-deleted rabies viruses for monosynaptic tracing and high-level gene expression in neurons. *Nature Protocols* **5,** 595–606 (2010).
43. Wickersham, I. R., Finke, S., Conzelmann, K. & Callaway, E. M. Retrograde neuronal tracing with a deletion-mutant rabies virus. *Nature Methods* **4,** 47–49 (2007).
44. Grimm, D. *et al.* In vitro and in vivo gene therapy vector evolution via multispecies interbreeding and retargeting of adeno-associated viruses. *J. Virol.* **82,** 5887–5911 (2008).
45. Lammel, S. *et al.* Input-specific control of reward and aversion in the ventral tegmental area. *Nature* **491,** 212–217 (2012).
46. Ben-Barak, Y., Russell, J., Whitnall, M., Ozato, K. & Gainer, H. Neurophysin in the hypothalamo-neurohypophysial system. I. Production and characterization of monoclonal antibodies. *J. Neurosci.* **5,** 81–97 (1985).
47. Whitnall, M. H., Key, S., Ben-Barak, Y., Ozato, K. & Gainer, H. Neurophysin in the hypothalamo-neurohypophysial system. II. Immunocytochemical studies of the ontogeny of oxytocinergic and vasopressinergic neurons. *J. Neurosci.* **5,** 98–109 (1985).

doi:10.1038/nature12518

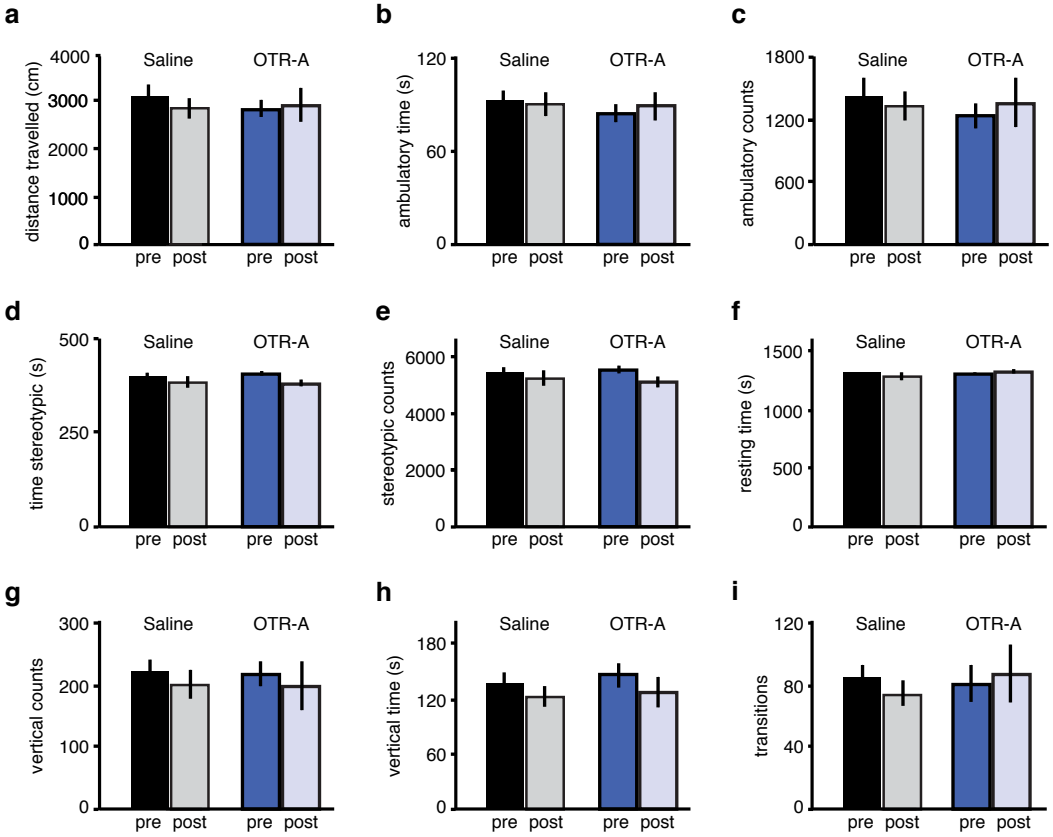

Supplementary Figure 1. Locomotor activity is not altered by sCPP or OTR-A. a, distance travelled is not different between groups (saline injected, pre 3116 ± 262, post 2865 ± 215, n = 18 animals, p = 0.450; OTR-A injected, pre 2862 ± 179, post 2936 ± 354, n = 15 animals, p = 0.848). **b,** ambulatory time is not different between groups (saline injected, pre 92 ± 7, post 90 ± 89, n = 18 animals, p = 0.830; OTR-A injected, pre 85 ± 6, post 89 ± 9, n = 15 animals, p = 0.687). **c,** ambulatory counts are not different between groups (saline injected, pre 1421 ± 184, post 1330 ± 142, n = 18 animals, p = 0.688; OTR-A injected, pre 1238 ± 122, post 1361 ± 232, n = 15 animals, p = 0.630). **d,** time stereotypic is not different between groups (saline injected, pre 397 ± 10, post 383 ± 15, n = 18 animals, p = 0.417; OTR-A injected, pre 402 ± 6, post 383 ± 11, n = 13 animals, p = 0.111). **e,** stereotypic counts are not different between groups (saline injected, pre 5362 ± 210, post 5226 ± 275, n = 18 animals, p = 0.689; OTR-A injected, pre 5453 ± 141, post 5133 ± 192, n = 13 animals, p = 0.174). **f,** resting time is not different between groups (saline injected, pre 1308 ± 14, post 1284 ± 36, n = 18 animals, p = 0.532; OTR-A injected, pre 1307 ± 12, post 1326 ± 18, n = 15 animals, p = 0.368). **g,** vertical counts are not different between groups (saline injected, pre 220 ± 18, post 200 ± 22, n = 18 animals, p = 0.466; OTR-A injected, pre 217 ± 20, post 197 ± 38, n = 11 animals, p = 0.628). **h,** vertical time is not different between groups (saline injected, pre 138 ± 11, post 123 ± 11, n = 18 animals, p = 0.346; OTR-A injected, pre 145 ± 13, post 127 ± 17, n = 11 animals, p = 0.384). **i,** number of transitions are not different between groups (saline injected, pre 85 ± 7, post 74 ± 8, n = 18 animals, p = 0.306; OTR-A injected, pre 81 ± 12, post 87 ± 19, n = 15 animals, 0.759). Summary data are presented as mean ± s.e.m (*$P < 0.05$).

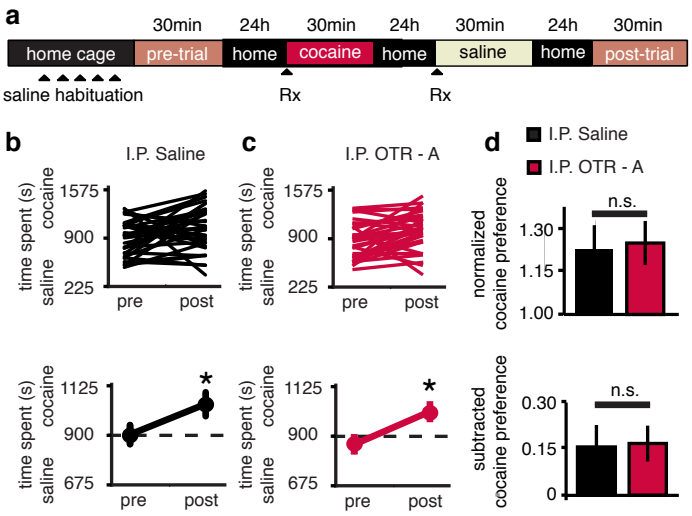

Supplementary Figure 2. Cocaine conditioned place preference (cCPP) does not require OT. a, Experimental time course for cocaine CPP. **b-c**, Individual (top) and average (bottom) responses in i.p. saline injected (**b**), versus i.p. OTR-A injected (**c**) animals. Both i.p. saline and i.p. OTR-A injected animals, spend more time in the cocaine context following conditioning (i.p. saline, pre 903 ± 43, post 1042 ± 54, $n = 34$ animals, p = 0.034 paired t-test; i.p. OTR-A, pre 863 ± 46, post 1011 ± 47, $n = 32$ animals, p = 0.007 paired t-test). **d**, Comparisons between i.p. saline versus i.p. OTR-A treated animals reveals no difference in normalized cocaine preference and subtracted cocaine preference in OTR-A treated animals (normalized saline 1.225 ± 0.079, OTR-A 1.245 ± 0.074, p = 0.906 unpaired t-test; subtracted saline 0.154 ± 0.069, OTR-A 0.165 ± 0.057, p = 0.857 unpaired t-test). Summary data are presented as mean ± s.e.m (*$P < 0.05$).

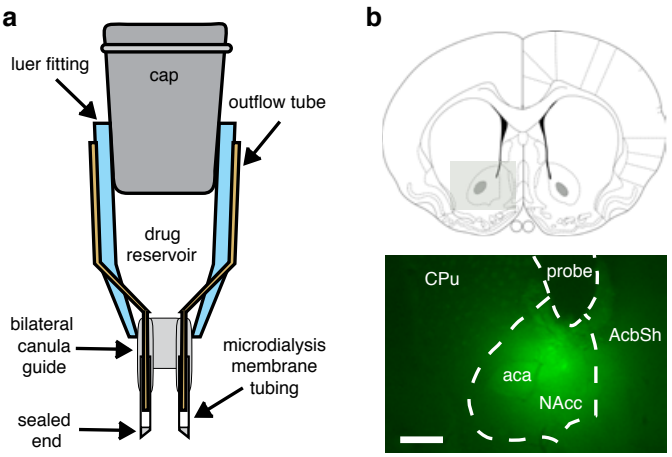

Supplementary Figure 3. Andalman reverse microdialysis probes. a, Schematic of Andalman probe for reverse microdialysis experiments in Fig. 1f-i and 5l-o. **b,** Post-hoc confirmation of probe placement and competency.

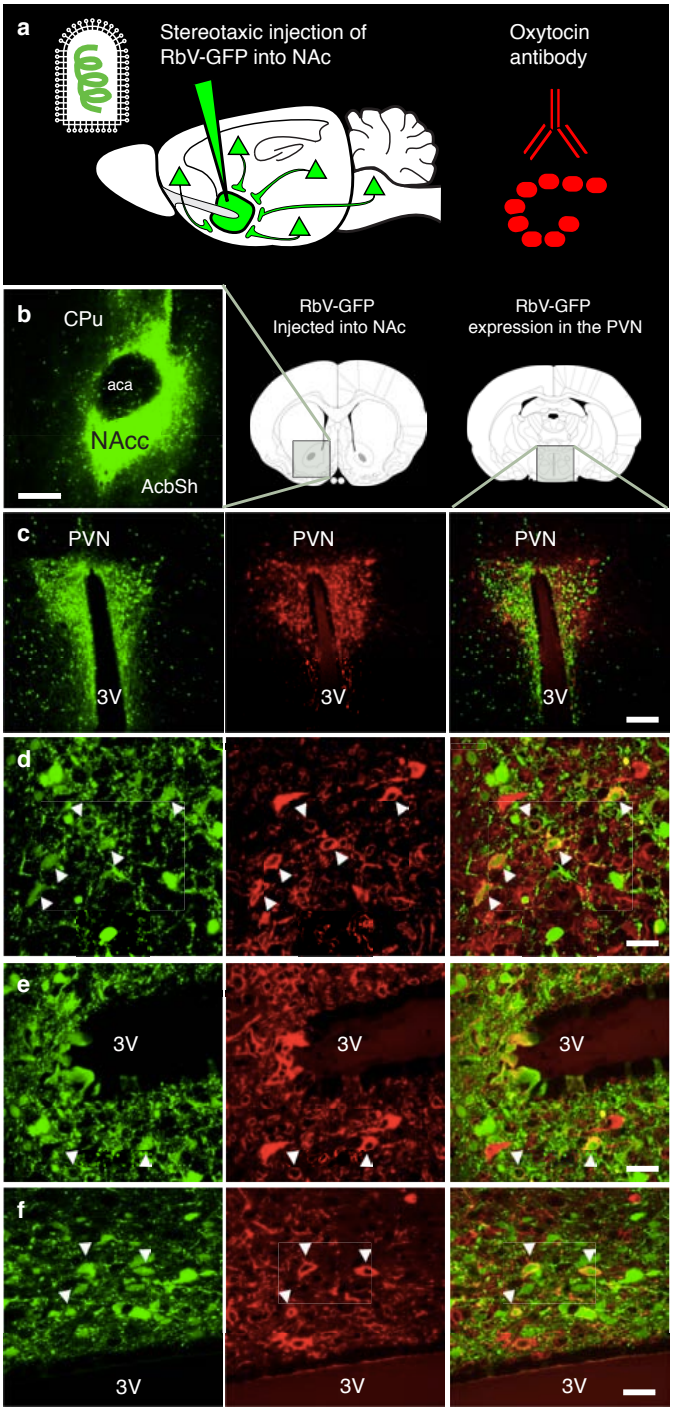

Supplementary Figure 4. OT expressing neurons in the paraventricular nucleus (PVN) send projections to the NAc. a, Diagram illustrating the injection of RbV-GFP into the NAc, followed by antibody labeling of OT producing neurons in the PVN. **b,** Localization and expression of RbV-GFP in the NAc **(**scale bars 200 µm). **c-f,** Low magnification (**c**,scale bar 100 µm) and high magnification **(d-f,** scale bars 20 µm) images of PVN cells that have been retrogradely labeled by RbV-GFP taken up by presynaptic terminals in the NAc (green, left panels) and labeled by ant-OT-np antibody (red, center panels). Co-localization (merged right panels) indicates oxytocinergic neurons that project to the NAc; arrowheads highlight individual cells that show co-localization. (Nucleus accumbens core, NAcc; nucleus accumbens shell, AcbSh; anterior commissure, aca; caudate putamen, CPu; third ventricle, 3V; paraventricular nucleus of the hypothalamus, PVN)

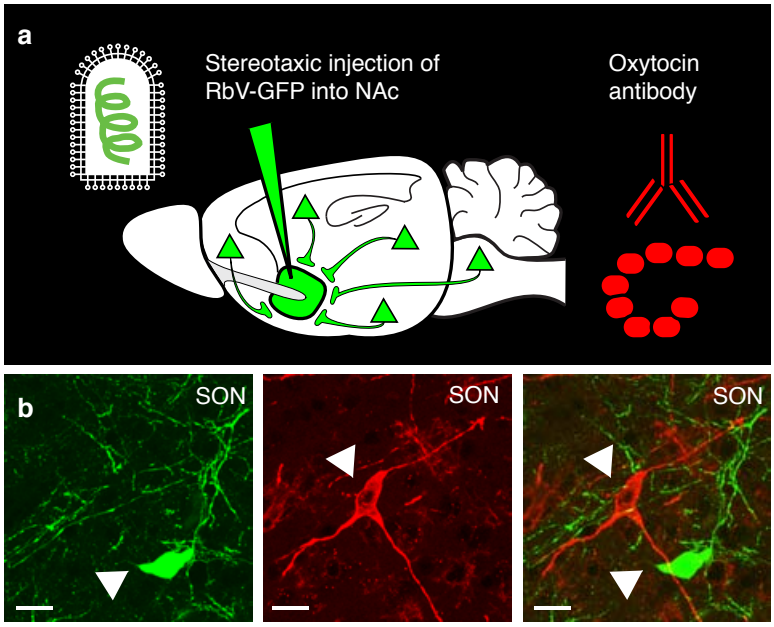

Supplementary Figure 5. OT expressing neurons in the Supraoptic Nucleus (SON) do not send projections to the NAc. a, Diagram illustrating the injection of RbV-GFP into the NAc, followed by antibody labeling of OT producing neurons in the SON. **b,** high magnification **(**scale bars 20 μm) images of SON cells that have been retrogradely labeled by RbV-GFP taken up by presynaptic terminals in the NAc (green, left panels) or labeled by ant-OT-np antibody (red, center panels). Absence of co-localization (merged right panels) indicates oxytocinergic neurons do not project to the NAc.

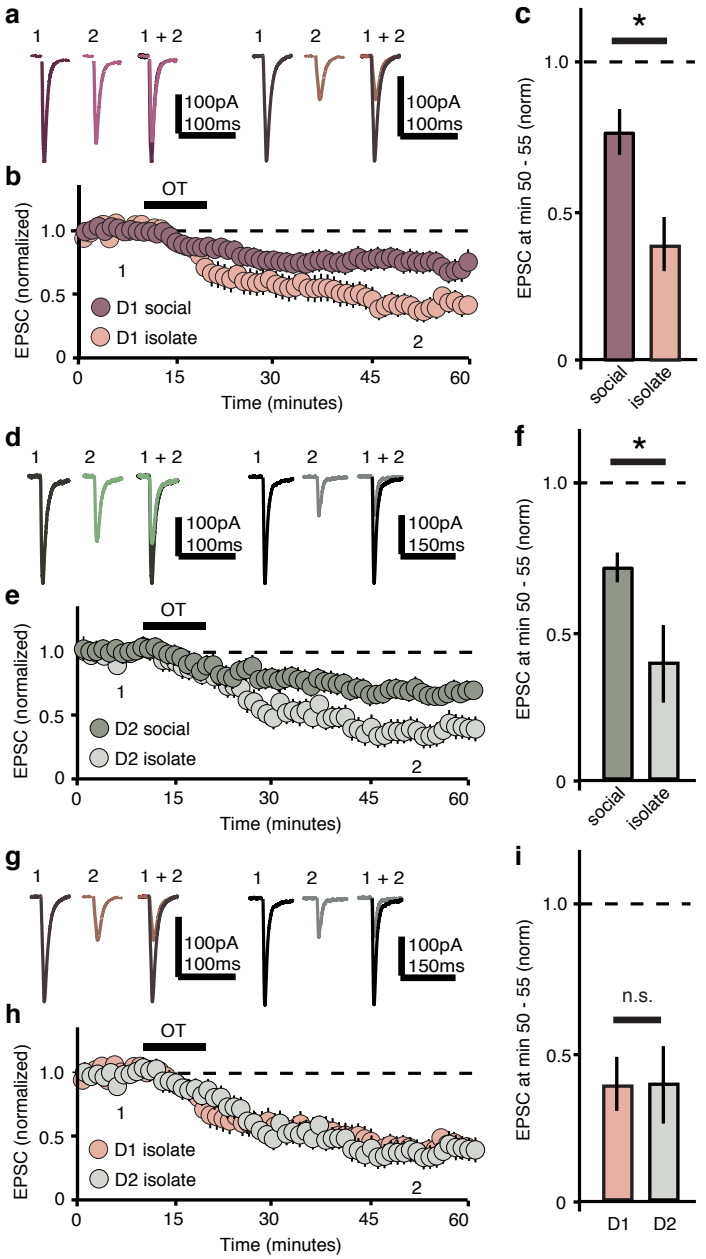

Supplementary Figure 6. Increased magnitude of OT-LTD in both D1 and D2 receptor expressing MSN following isolation conditioning. a-h, Representative traces **(a,d,g)**, summary time course **(b,e,h),** and average post-treatment magnitude comparisons **(c,f.i)** reveal that the magnitude of OT-LTD is significantly increased in both D1 **(a-c)** and D2 **(d-f)** cells from isolation versus socially reared animals (D1 isolation, 0.379 ± 0.090, n = 6 cells and D1 social, 0.756 ± 0.078, n = 9 cells, p = 0.00524 unpaired t-test; D2 isolation, 0.386 ± 0.129, n = 5 and D2 social, 0.708 ± 0.051, n = 11 cells, p = 0.00845 unpaired t-test); and the magnitude of EPSC OT-LTD is not different in D1 versus D2 MSNs from slices made from isolation conditioned animals (**g-i**) (p = 0.957 unpaired t-test). Representative traces are binned from 5 consecutive sweeps taken at times indicated (1 and 2). Summary data are presented as mean ± s.e.m (*$P < 0.05$).

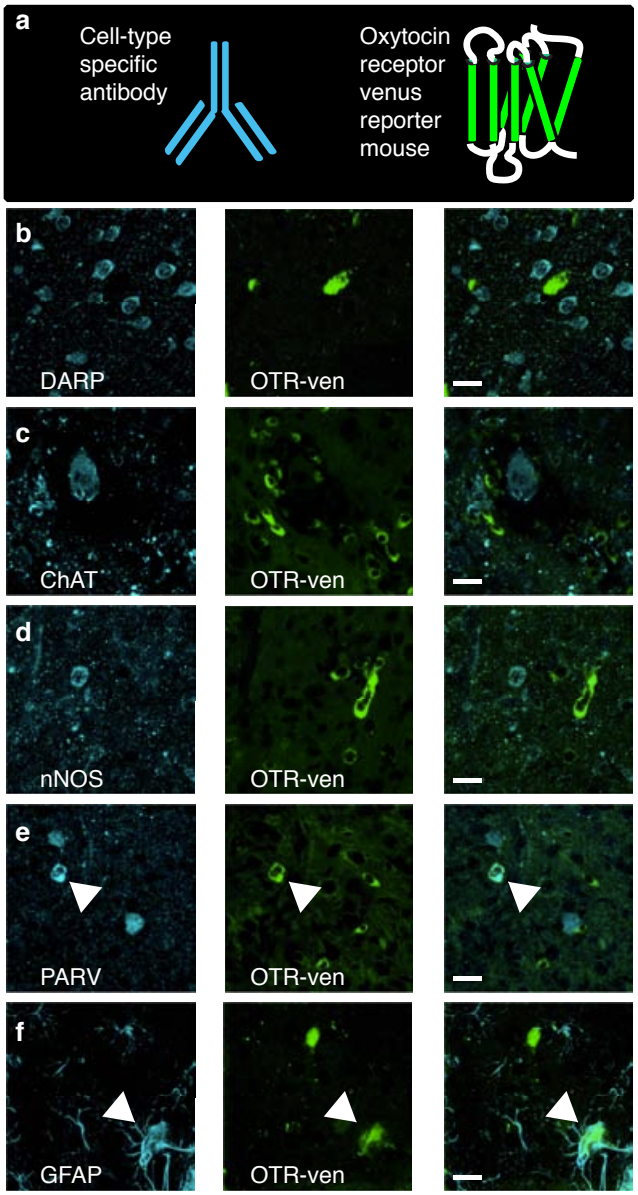

Supplementary Figure 7. OT receptor (OTR) expressing cells in the NAc. **a,** Diagram illustrating immunolabeling with cell-type specific antibodies in the NAc of OTR-Venus mice. **b,** DARP positive MSNs (blue, left) and OTR-Ven positive cells (green, center) do not co-localize (merge, right). **c,** CHAT positive cholinergic interneurons (blue, left) and OTR-Ven positive cells (green, center) do not co-localize (merge, right). **d,** nNOS positive inhibitory interneurons (blue, left) and OTR-Ven positive cells (green, center) do not co-localize (merge, right). **e,** a subset of PARV positive inhibitory interneurons (blue, left) and OTR-Venus positive cells (green, center) show co-localization (merge, right). **f,** a subset of GFAP positive glial cells (blue, left) and OTR-Ven positive cells (green, center) show co-localization (merge, right). (Scale bars 20 μm)

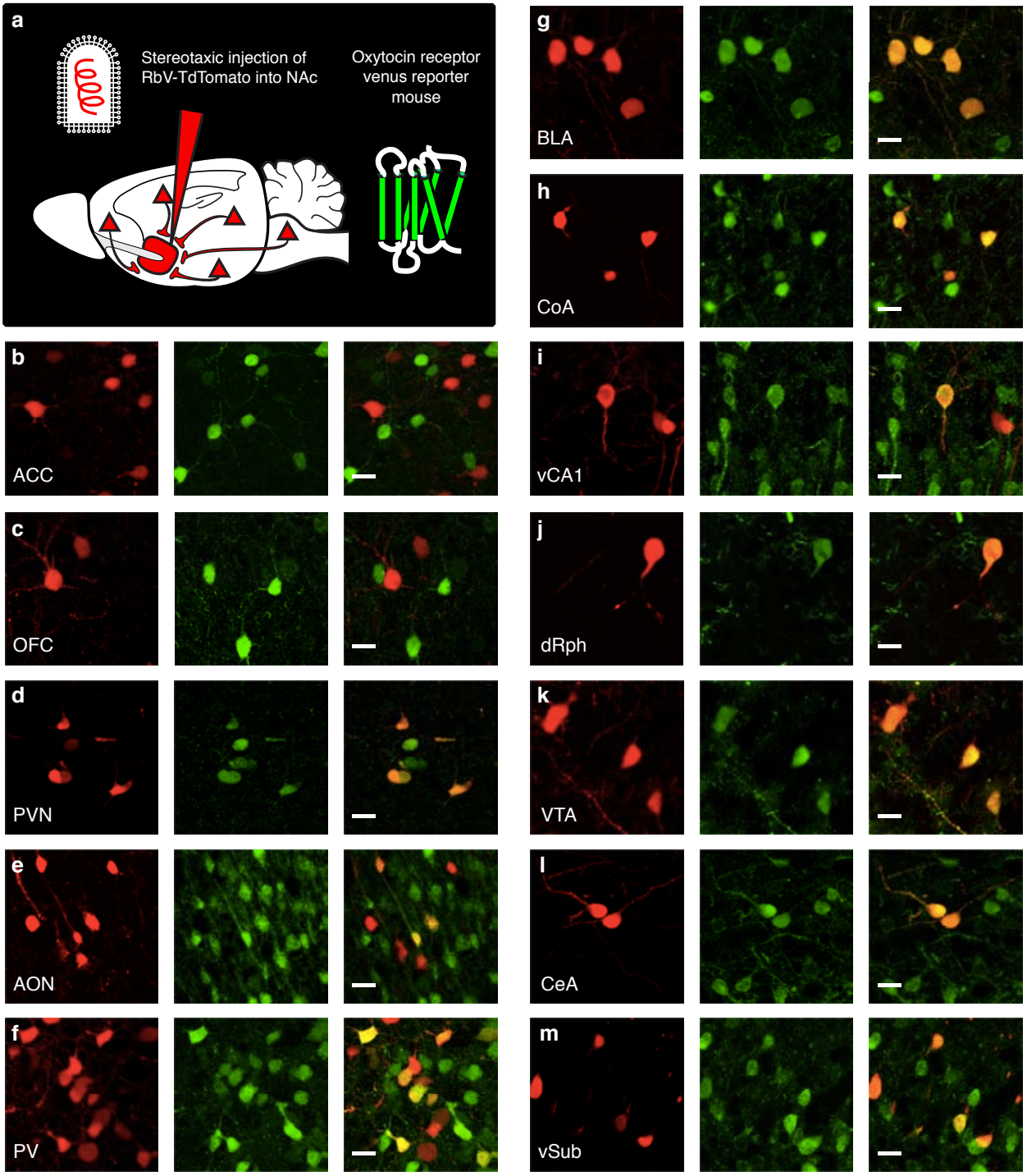

Supplementary Figure 8. OT receptor expressing cells that project to the NAc. a, Diagram illustrating stereotaxic injection of RbV-TdTomato into the NAc of OTR-Venus mice. **b-m,** high magnification images of cells in the (b) anterior cingulate cortex, ACC; (c) orbitofrontal cortex, OFC; (d) paraventricular nucleus of the hypothalamus, PVN; (e) anterior olfactory nucleus, AON; (f) paraventricular thalamus, PV; (g) basolateral amygdala, BLA; (h) cortex of the amygdala, CoA; (i) ventral hippocampal CA1, vCA1; (j) dorsal Raphe nucleus, dRph; (k) caudal ventral tegmental nucleus, VTA; (l) central amygdala, CeA; and ventral subiculum, vSub that have been retrogradely labeled by RbV-GFP taken up by presynaptic terminals in the NAc (red, left panels) and that express OTR-Venus (green, center panels). Co-localization (merge, right panels) is notably absent in (b) ACC and (c) OFC, but in all other regions (d-m), a subset of cells show clear co-localization (project to the NAc and express OTR-Venus), implicating these neurons as a putative source of presynaptic OTRs in the NAc. (Scale bars 20 μm).

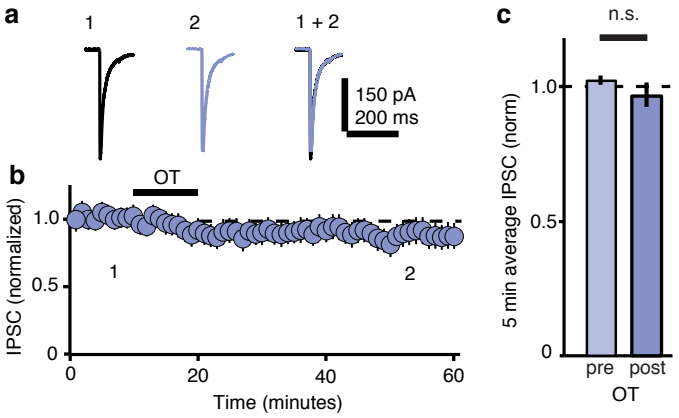

Supplementary Figure 9. OT does not alter inhibitory postsynaptic currents (IPSCs) recorded from NAc MSNs. Representative traces **(a)**, summary time course **(b)** and average post-treatment magnitude comparisons **(c)** reveal absence of significant OT-induced changes in IPSC amplitude (pre 1.023 ± 0.0186, post 0.962 ± 0.0456, n = 11 cells, p = 0.557 paired t-test). Representative traces are binned from 5 consecutive sweeps taken at times indicated (1 and 2). Summary data are presented as mean ± s.e.m (*$P < 0.05$).

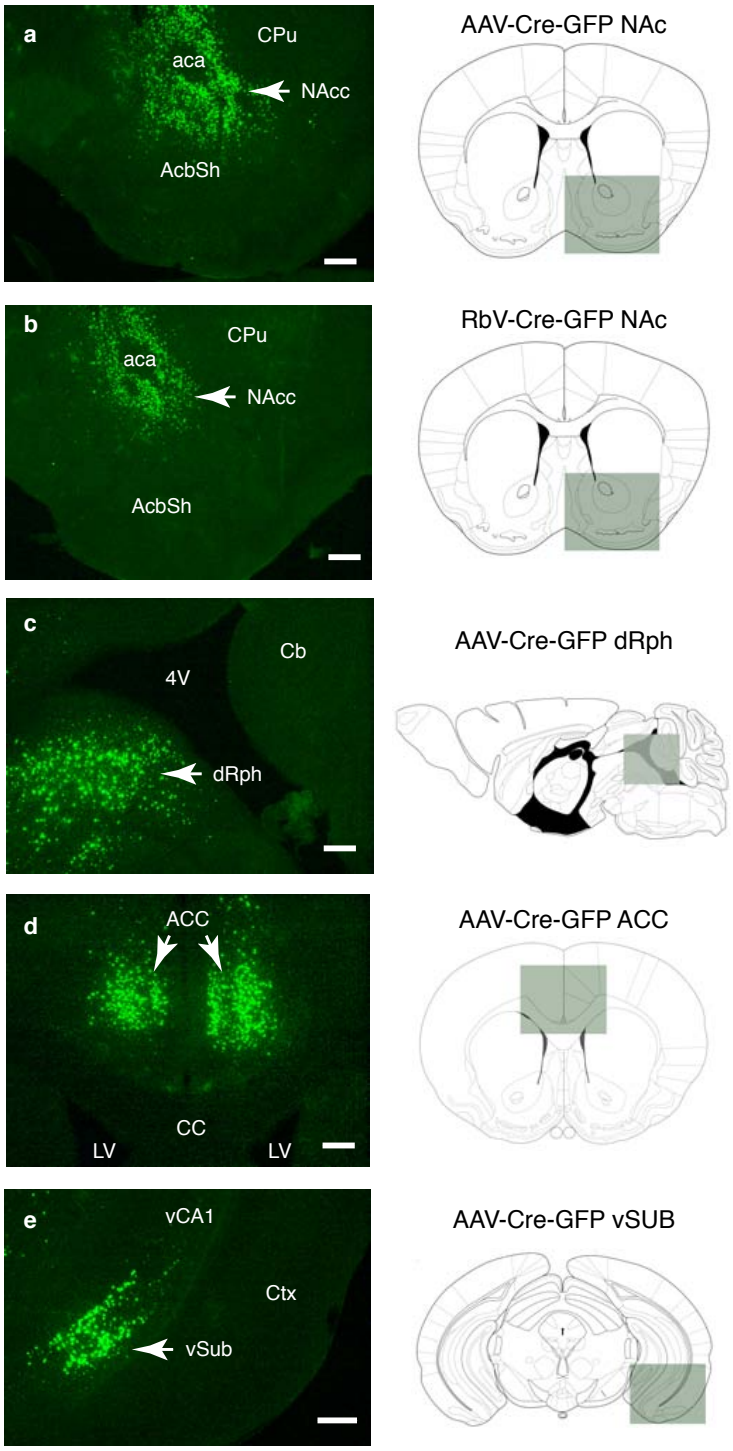

Supplementary Figure 10. Post-hoc confirmation of viral injection sites and transgene expression. a,b Localization and expression of (**a**) AAV-Cre-GFP and **(b)** RbV-Cre-GFP stereotaxic injections into the NAc. **c,d,e**, Localization and expression of AAV-Cre-GFP stereotaxic injections into the (**c**) dRph, (**d**) ACC and (**e**) vSub. (Nucleus accumbens core, NAcc; nucleus accumbens shell, AcbSh; anterior commissure, aca; caudate putamen a.k.a. dorsal striatum, CPu; dorsal Raphe, dRph; fourth ventricle, 4V; cerebellum, Cb; anterior cingulate cortex, ACC; corpus callosum, CC; lateral ventricle, LV; ventral subiculum, vSub; ventral CA1 region of the hippocampus, vCA1; entorhinal cortex, Ctx; Scale bars 250 µm)

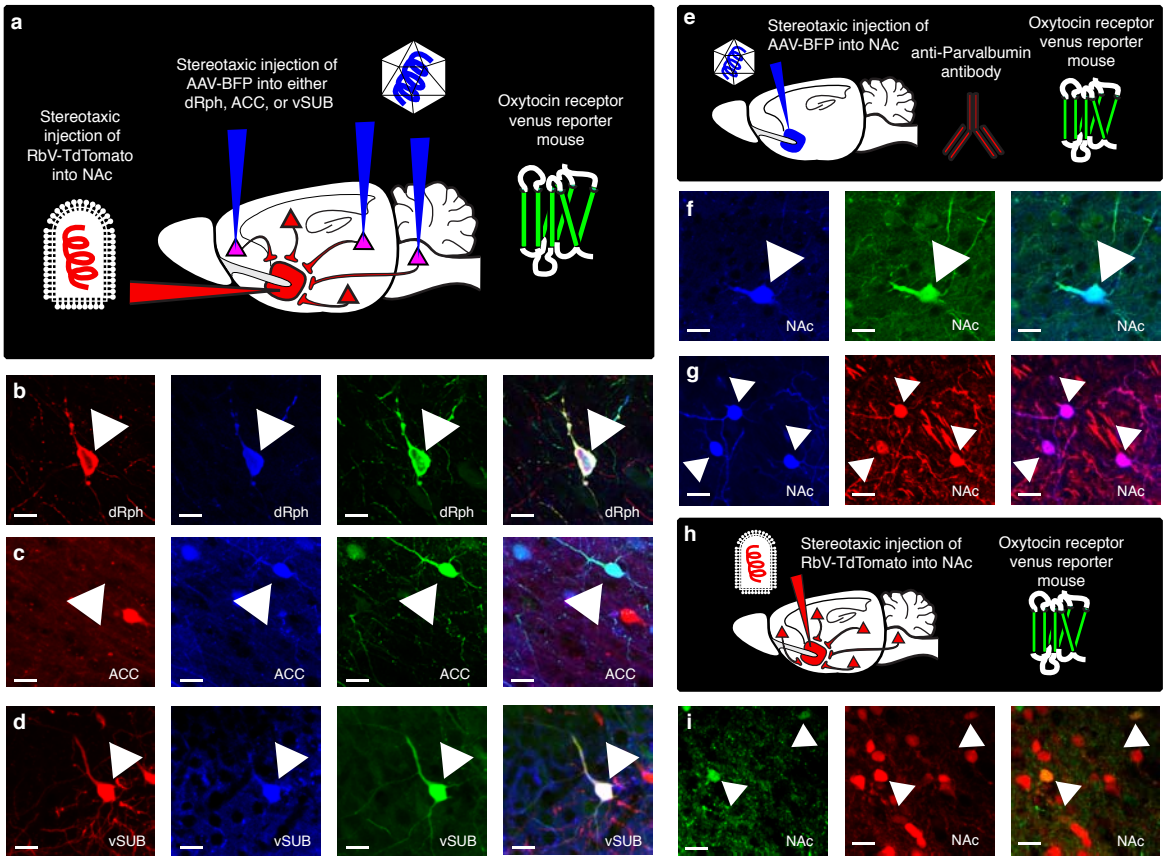

Supplementary Figure 11. Confirmation of viral tropism for OTR-expressing and NAc-projecting cells. a, Diagram illustrating stereotaxic injection of RbV-TdTomato into the NAc of OTR-Venus mice followed by AAV-BFP expression in either dorsal Raphe nucleus, dRph, anterior cingulate cortex, ACC or ventral subiculum, vSub shown in (**b-d**). **b-d,** high magnification images of cells in the (b) dRpH (c) ACC or (d) vSUB that have been retrogradely labeled by RbV-GFP taken up by presynaptic terminals in the NAc (red, left panels), labeled by local infection with AAV-BFP (blue, center left), and that express OTR-Venus (green, center right panels). Clear co-localization (merge, right panels) between RbV-TdTomato, OTR-Venus and AAV-BFP is evident in (b and d) and co-localization between OTR-Venus and AAV-BFP is evident (c). **e,** Diagram illustrating stereotaxic injection of AAV-BFP into the NAc of OTR-Venus mice or WT mice followed by subsequent immunohistochemistry with anti-Parvalbumin antibody shown in (**f-g**). **f,** Local infection with AAV-BFP (blue, left) in cells that express OTR-Venus (green, center). Co-localization (merge, right) indicates AAV tropism for OTR expressing cells in the NAc. **g,** Local infection with AAV-BFP (blue, left) in cells that express Parvalbumin (red, center). Co-localization (merge, right) indicates AAV tropism for Parvalbumin expressing cells in the NAc. **h,** Diagram illustrating stereotaxic injection of RbV-TdTomato into the NAc of OTR-Venus mice shown in (i). **i,** Local infection with RbV-TdTomato (red, left) in cells that express OTR-Venus (green, center). Co-localization (merge, right) indicates RbV tropism for OTR expressing cells in the NAc. (Scale bars 20 µm).

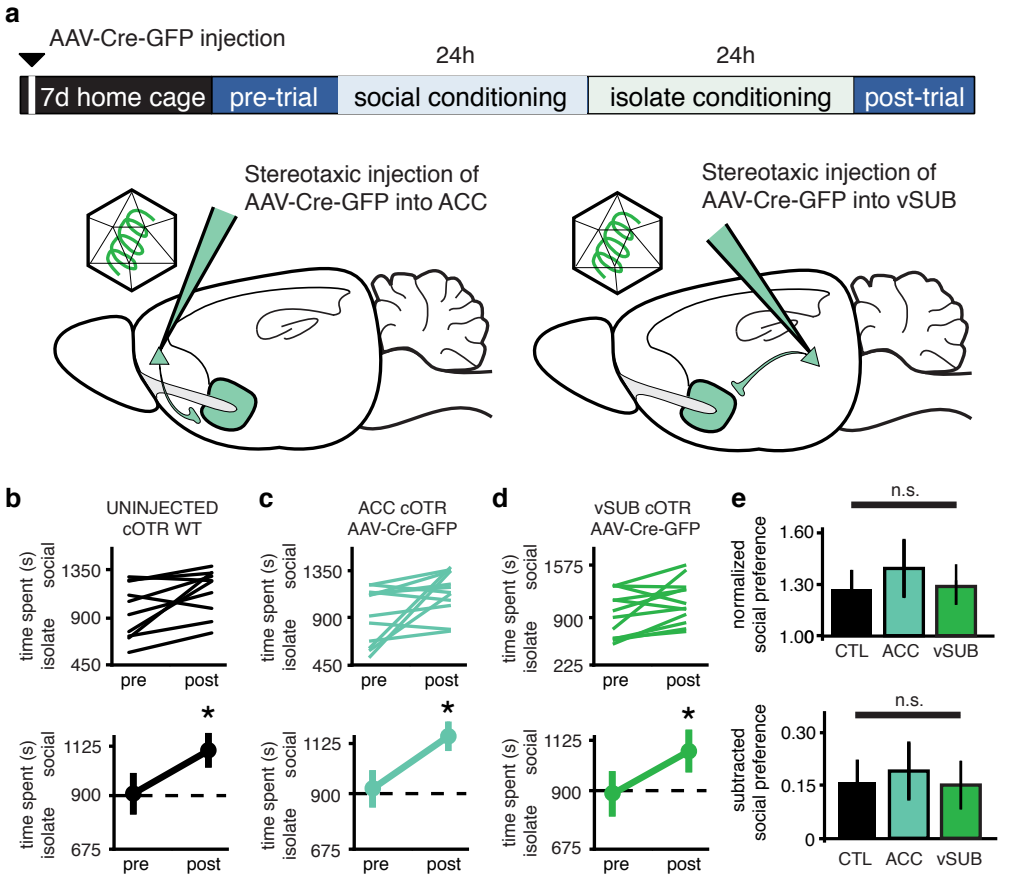

Supplementary Figure 12. ACC and vSub OT receptors (OTRs) are not required for sCPP. a, Diagram illustrating time course of viral injections into the ACC and vSub for sCPP experiments in **b-e**. **b,c,d** Individual (top) and average (bottom) preference scores indicate that un-injected cOTR KO animals (**b**), cOTR KO animals injected with AAV-Cre-GFP into the ACC (**c**) and cOTR KO animals injected with AAV-Cre-GFP into the vSub (**d**) have increased preference for the social bedding cue after conditioning (un-injected cOTR KO, pre 935 ± 82, post 1151 ± 68, n = 10, p = 0.044 paired t-test; cOTR KO AAV-Cre-GFP ACC, pre 935 ± 78, post 1160 ± 61, n = 12, p = 0.034; cOTR KO AAV-Cre-GFP vSub, pre 907 ± 90, post 1085 ± 85, n = 12, p = 0.043). **e**, Comparisons between un-injected cOTR KO versus cOTR KO animals injected with AAV-Cre-GFP into the ACC or vSub reveals no difference in normalized social preference and subtracted social preference (normalized uninjected 1.250 ±0.095, cOTR KO AAV-Cre-GFP ACC 1.362 ± 0.166, cOTR KO AAV-Cre-GFP vSub 1.271 ± 0.124, p = 0.812, ANOVA; subtracted uninjected 0.212 ± 0.078, cOTR KO AAV-Cre-GFP ACC 0.251 ± 0.104, cOTR KO AAV-Cre-GFP vSub 0.199 ± 0.087, p = 0.912, ANOVA). Summary data are presented as mean ± s.e.m (*$P < 0.05$).

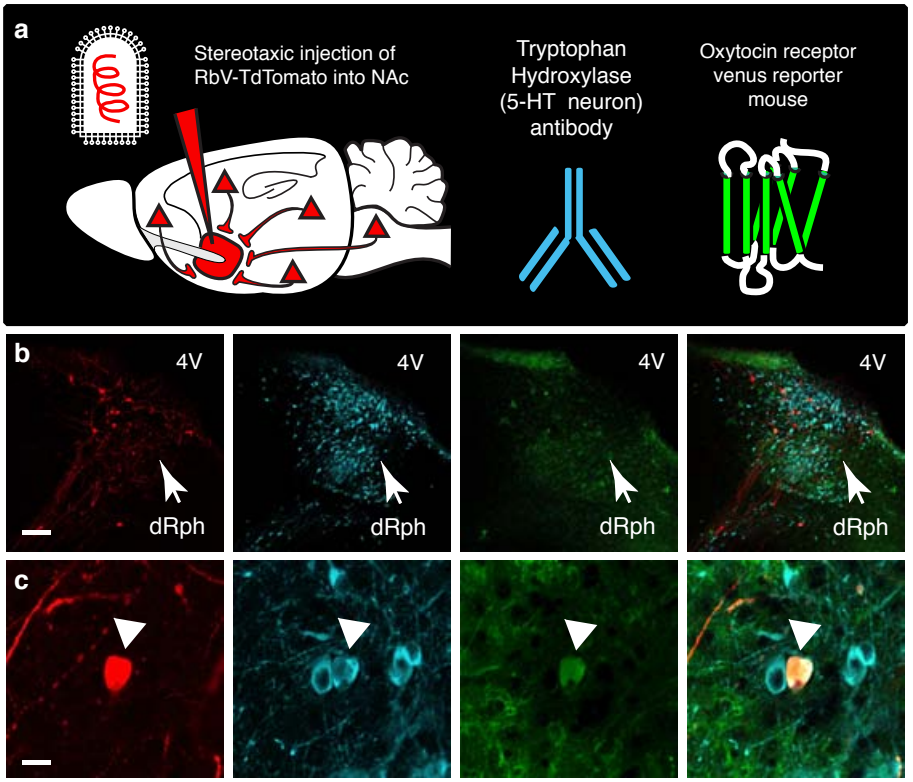

Supplementary Figure 13. OT receptor-expressing cells in the dRph send serotonergic projections to the NAc. a, Diagram illustrating stereotaxic injection of RbV-TdTomato into the NAc of OTR-Venus reporter mice, followed by subsequent immunohistochemistry with anti-tryptophan hydroxylase antibodies to label serotonergic neurons of the dRph. **b,c,** Low magnification (**b**, scale bar 200 µm) and high magnification (**c**, scale bar 20 µm) images of neurons in the dRph that send projections to the NAc (red, left), express OTR (green, middle left) and produce 5-HT (blue, middle right). Arrowheads and merged image (right) shows subset of neurons that show colocalization. (dorsal raphe, dRph; fourth ventricle, 4V).

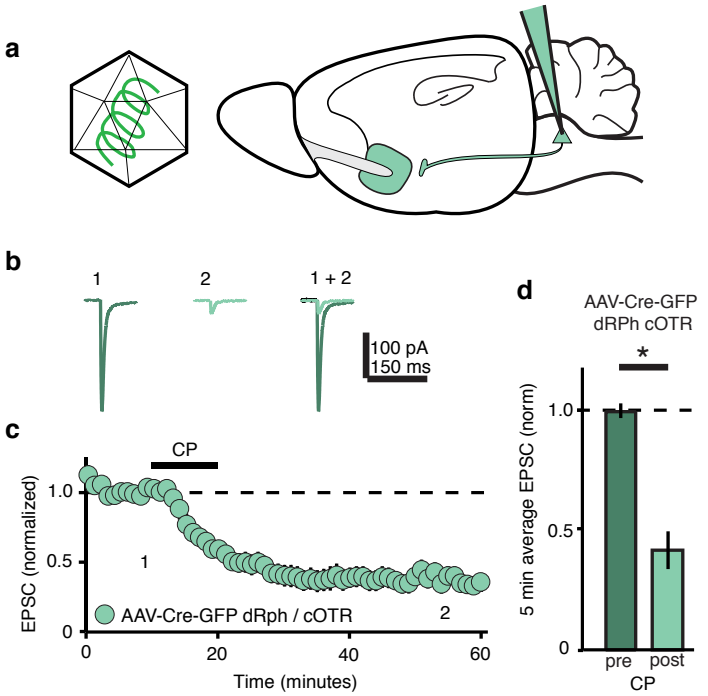

Supplementary Figure 14. Molecular ablation of OTRs in dorsal raphe does not disrupt 5HTR1b agonist induced LTD. a, Diagram illustrating time course of viral injections into the dRph for LTD experiments in **b-d**. Representative traces **(b)**, summary time course **(c)** and average post-treatment magnitude comparisons **(d)** reveal 5HT1b induced-LTD in EPSCs recorded from cOTR animals whose OTRs had been molecularly ablated by AAV-Cre-eGFP dRph injection (dRph-AAV-Cre-eGFP injected cOTR, pre 1.0158 ± 0.0315, post 0.3566 ± 0.0891, n = 5 cells, p = 0.0031 paired t-test). Representative traces are binned from 5 consecutive sweeps taken at times indicated (1 and 2). Summary data are presented as mean ± s.e.m (*$P < 0.05$).

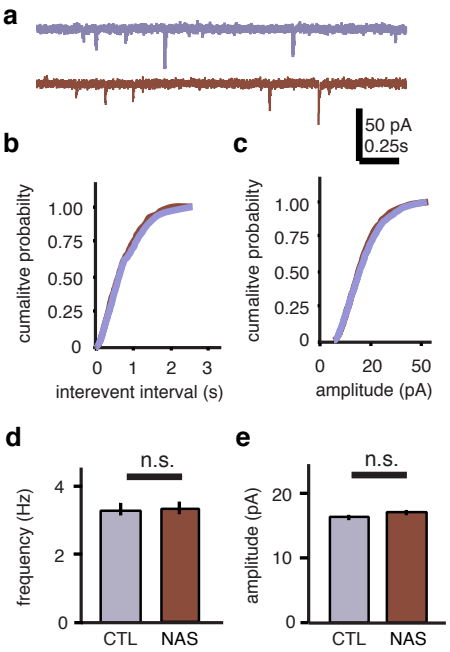

Supplementary Figure 15. 5HTR1b-A alone does not alter mini EPSC frequency or amplitude. a, Representative miniature EPSCs (mEPSCs) recorded in control neurons (purple) and neurons treated with NAS-181 (red, 20 µM, 10 minutes). **b**, Cumulative probability (top) and average (bottom) mEPSC frequency is not decreased in NAS-treated cells compared to control cells (control 3.31± 0.456, n = 10 cells, NAS-181 3.36 ± 0.409, n = 10 cells; p = 0.9346 unpaired t-test). **c**, Cumulative probability (top) and average (bottom) mEPSC amplitude is not different in NAS-treated cells compared to control cells (control 16.13 ± 1.152, n = 10 cells, NAS-181 16.90 ± 0.886, n = 10 cells; p = 0.5826 unpaired t-test). Summary data are presented as mean ± s.e.m (*$P < 0.05$).

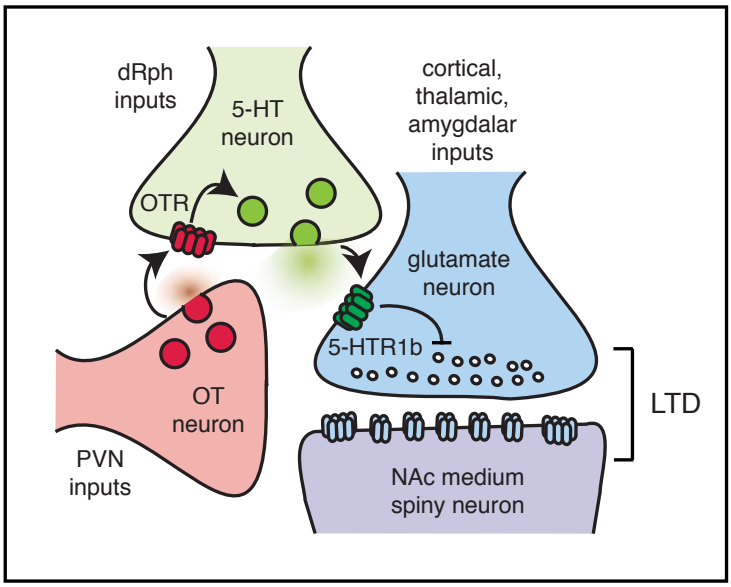

Supplementary Figure 16. Diagram illustrating model for induction of OT-induced LTD in NAc. OT producing neurons from the PVN release OT into the NAc. Activation of OTRs on presynaptic terminals of 5-HT neurons from the dRph causes the release of 5-HT into the NAc. Activation of 5HT1b receptors on glutamatergic terminals from various brain regions (cortex, amygdala, thalamus) decrease presynaptic function at excitatory synapses onto MSNs.